Southeastern Geology: Volume 28, No. 4
May 1988

Edited by: S. Duncan Heron, Jr.

Abstract

Academic journal published quarterly by the Department of Geology, Duke University.

SOUTHEASTERN GEOLOGY

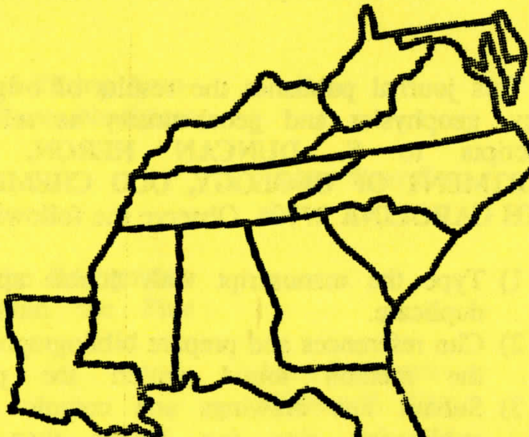

PUBLISHED AT DUKE UNIVERSITY DURHAM, NORTH CAROLINA

VOL. 28, NO. 4 MAY 1988

SOUTHEASTERN GEOLOGY

PUBLISHED QUARTERLY

AT

DUKE UNIVERSITY

Editor in Chief:
S. Duncan Heron, Jr.

Managing Editor:
James W. Clarke

This journal publishes the results of original research on all phases of geology, geophysics and geochemistry as related to the Southeast. Send manuscripts to **S. DUNCAN HERON, JR., DUKE UNIVERSITY, DEPARTMENT OF GEOLOGY, OLD CHEMISTRY BUILDING, DURHAM, NORTH CAROLINA 27706.** Observe the following:

1) Type the manuscript with double space lines and submit in duplicate.
2) Cite references and prepare bibliographic lists in accordance with the method found within the pages of this journal.
3) Submit line drawings and complex tables reduced to final publication size (no bigger than 8 x 5 1/8 inches).
4) Make certain that all photographs are sharp, clear, and of good contrast.
5) Stratigraphic terminology should abide by the North American Stratigraphic Code (Am. Assoc. Petroleum Geologists Bulletin, v. 67, p. 841-875).

Subscriptions to *Southeastern Geology* are $11.00 per volume (US and Canada), $13.00 per volume (foreign). Inquires should be sent to: **SOUTHEASTERN GEOLOGY, DUKE UNIVERSITY, DEPARTMENT OF GEOLOGY, OLD CHEMISTRY BUILDING, DURHAM, NORTH CAROLINA 27706.** Make checks payable to: *Southeastern Geology*.

SOUTHEASTERN GEOLOGY

Table of Contents

Vol. 28, No. 4

May 1988

1. Possible Active Fault Zones in West Tennessee Interpreted from Surface Lineaments and Magnetic and Gravity Anomalies — Douglas E. Wyatt, Jr., Richard G. Stearns — 191

2. Evidence of Quaternary Ground Tilting Associated with the Reelfoot Rift Zone, Northeast Arkansas — Randel Tom Cox — 211

3. Corona Structures: Key to the Recognition of Grenville Basement Within the Pine Mountain Window, Georgia — Alice L. Stieve, William B. Size — 225

4. Biont Transition Sequences in the Johnson Point *Crepidula* Biostrome, Early Pleistocene of North Carolina — William Miller, III — 237

POSSIBLE ACTIVE FAULT ZONES IN WEST TENNESSEE INTERPRETED FROM SURFACE LINEAMENTS AND MAGNETIC AND GRAVITY ANOMALIES

DOUGLAS E. WYATT, JR. *7639 Whites Creek Pk., Joelton, TN 37080*

RICHARD G. STEARNS *Geology Department, Vanderbilt University, Nashville, TN, 37235*

ABSTRACT

There are fourteen swarms of lineaments that are at least 20 miles long and are also parallel to nearby elongated gravity and magnetic anomalies. This paper explores the possibility that these "lines" could be fracture traces marking fault zones. One of these lines along Chickasaw Bluff near the Kentucky-Tennessee border has previously-known faults throughout its length, and another (Rives Line) has a short mapped surface fault at its NE end. These two, with another called the Bluff line, are the NE-trending "Big Creek Fault Zone" of Fisk (1944). Two NW-trending lines have evidence of faulting. Offset of the earthquake swarm occurs along the Dyersburg line near Caruthersville, Missouri, and the Humboldt line coincides with a magnetic basement low that could be a graben.

Surface lineaments trending parallel to both gravity and magnetic lineaments are abundant in azimuths 30-69° and 130-159°, and these azimuths include the direction of the 14 lines. The 30-69° trend contains the approximate 50° trend of the Mississippi Valley graben, the direction 159° is the approximate trend of the low density crust mapped by Hildebrand in 1985, and 130° is the approximate trend of the pre-Cretaceous Pascola arch. A belt of sparse topographic and magnetic lineaments trends ESE parallel to the Pascola Arch.

INTRODUCTION

West Tennessee includes part of the Mississippi Valley graben. This graben is associated with the Reelfoot Rift, a main feature of the New Madrid earthquake region (Figure 1). It would be useful to locate young faults in and near the graben, because they could be earthquake sources. Direct observation of surface fractures would help, but the land surface consists of unconsolidated Cretaceous to Recent sediment, commonly weathered and covered by vegetation, so exposed fractures are rare.

One case where a fault is expressed at the surface is a 35-mile stretch of the prominent straight Chickasaw Bluff (the east side of the Mississippi River alluvial plain) across the Tennessee-Kentucky border. This is the only example in the region where lengthy faults have been independently mapped to coincide with a long straight surface feature. Its existence is a main support of the hypothesis that other straight surface features may mark faults in this area.

Rivers that empty into the south-flowing Mississippi flow northwestward at an obtuse angle to the flow of the Mississippi, and long straight reaches are

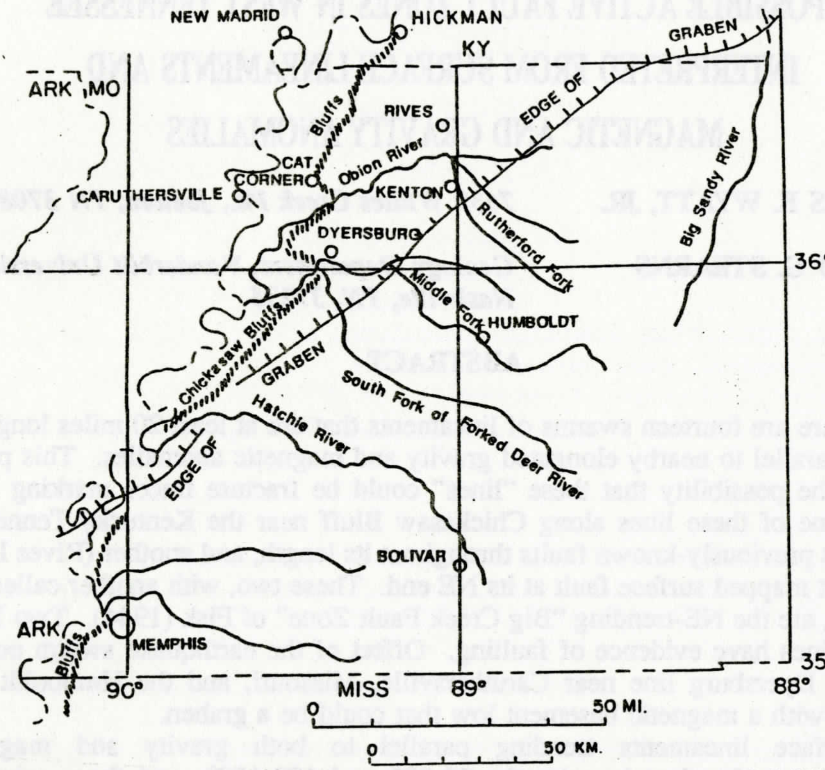

Figure 1. Location map for the study area. Notice the nearly parallel NW flowing rivers. Hatchures mark Chickasaw Bluff. The edge of the Mississippi Valley Graben (a main structure of the Reelfoot Rift) is from Hildenbrand and others (1982).

common. Straight streams that follow such a rectilinear pattern may be controlled by fractures and perhaps straight stream segments flowing in other directions are also controlled by fractures.

This investigation is an attempt to relate surface lineaments to buried features, and so discover the surface lineaments that are most likely to relate to buried faults. Surface lineaments can be viewed and interpreted alone, but our working hypothesis is that in cases where surface lineaments are parallel to nearby geophysical lineaments, those lineaments are more likely to be fracture traces or even parts of active fault zones. Surface lineaments, (possibly fracture traces) were obtained from topographic maps and a Landsat image. Linear trends that reflect buried rocks were drawn from trends of gravity and magnetic anomalies.

PREVIOUS INVESTIGATIONS OF LINEAR SURFACE FEATURES

H.N. Fisk in 1944 used aerial photographs at a large scale to study the entire lower Mississippi Valley. Several of his lineaments are parts of larger features he called "fault zones" (Figure 2). He concluded that many Chickasaw Bluff segments in West Tennessee are faults and classed them as parts of the "Big Creek Fault Zone" that extends for more than 300 miles from Louisiana to Kentucky.

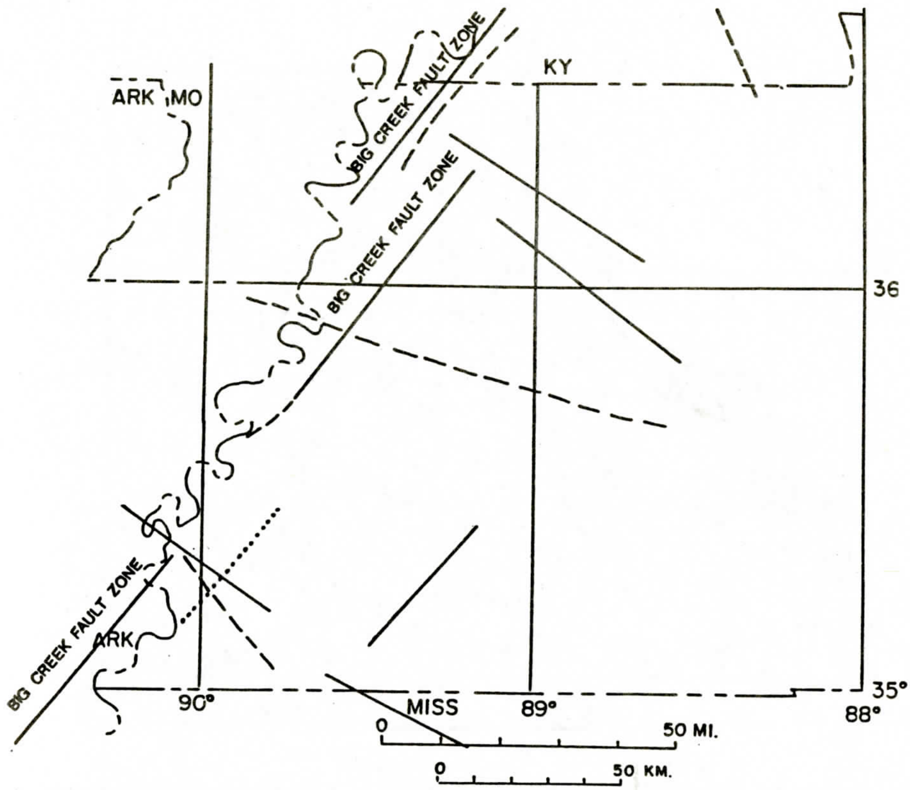

Figure 2. Surface lineaments published by previous investigators. The solid lines are from Fisk (1944); the dashed lines are from Hildenbrand, Kane and Hendricks (1982). One dotted line is from O'Leary and Simpson (1977).

Later workers have been highly selective as to which lineaments in Fisk's "fault zones" they considered likely to be faults.

Stearns and Wilson (1972) mapped lineaments from 7 1/2-minute topographic quadrangles in West Tennessee. They did not consider most of these to be faults, rather joints whose abundance relate to faulting. Some of these are used for this study. O'Leary and Simpson (1977) published one lineament in our study area near the Mississippi River (Figure 2).

Argialas (1979) mapped 590 lineaments from Landsat images in West Tennessee and compared them with 133 lineaments from a regional gravity map. He concluded that lineaments trend NE and SE with secondary NS and EW trends. He reported trends with about 40-60° and about 120-150° azimuths from Landsat lineaments, and about a 30-70° azimuth for NE gravity with a more irregular spread of SE gravity. This investigation verifies and adds some detail to his results by showing that his conclusions generally hold for lineaments from topographic maps and from magnetic anomalies.

Hildenbrand, Kane and Hendricks (1982) showed several magnetic lineaments in West Tennessee, including some trending northwestward parallel to those we will emphasize. They also mapped the edge of the Mississippi Valley Graben (part of Reelfoot Rift) as estimated from magnetic trends. Hildenbrand (1985)

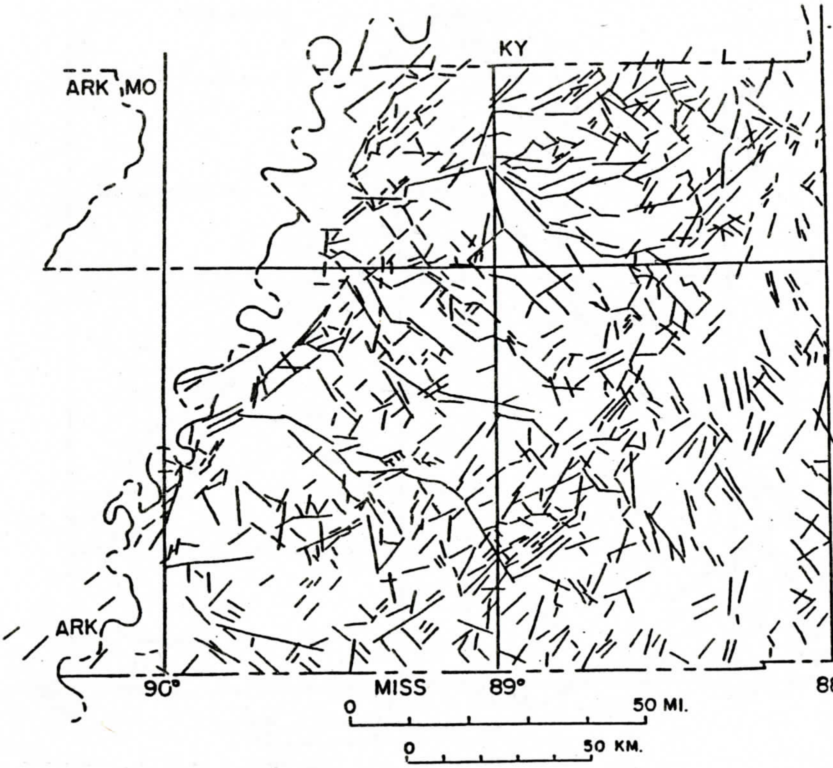

Figure 3. Surface lineaments. Most are from a Landsat image and two AMS topographic maps. To these are added lineaments from 7 1/2-minute topographic quadrangles by Stearns and Wilson (1972).

mapped a belt of low density anomalous crust that trends SSE and will be shown to relate to surface lineaments in this paper.

The data base used in our study was generated by Wyatt (1985).

METHODS AND DATA USED

Lineaments, Swarms, Lines, and Cells

A lineament is "a mappable feature, and if segmented, its parts align in a straight or gently curvilinear pattern differing from the surrounding areas" (O'Leary and others, 1976). We drew both surface lineaments and geophysical lineaments. We did not map segmented lineaments; rather, the term "swarm" is used as a collective term to describe a grouping of end-to- end (segmented) or closely parallel lineaments. The term "line" is used for swarms that the writers believe merit a name (e. g. Dyersburg line). Cells are 30-minute quadrangle subareas of our study region, within which lineaments can be compared locally. We made our most detailed comparisons in six cells; four are adjacent to the Kentucky border from 88° into Missouri, and the two others are the next tier south from 89° into Arkansas. A 30-minute cell size was necessary to have a sufficient number of geophysical lineaments for a meaningful correlation.

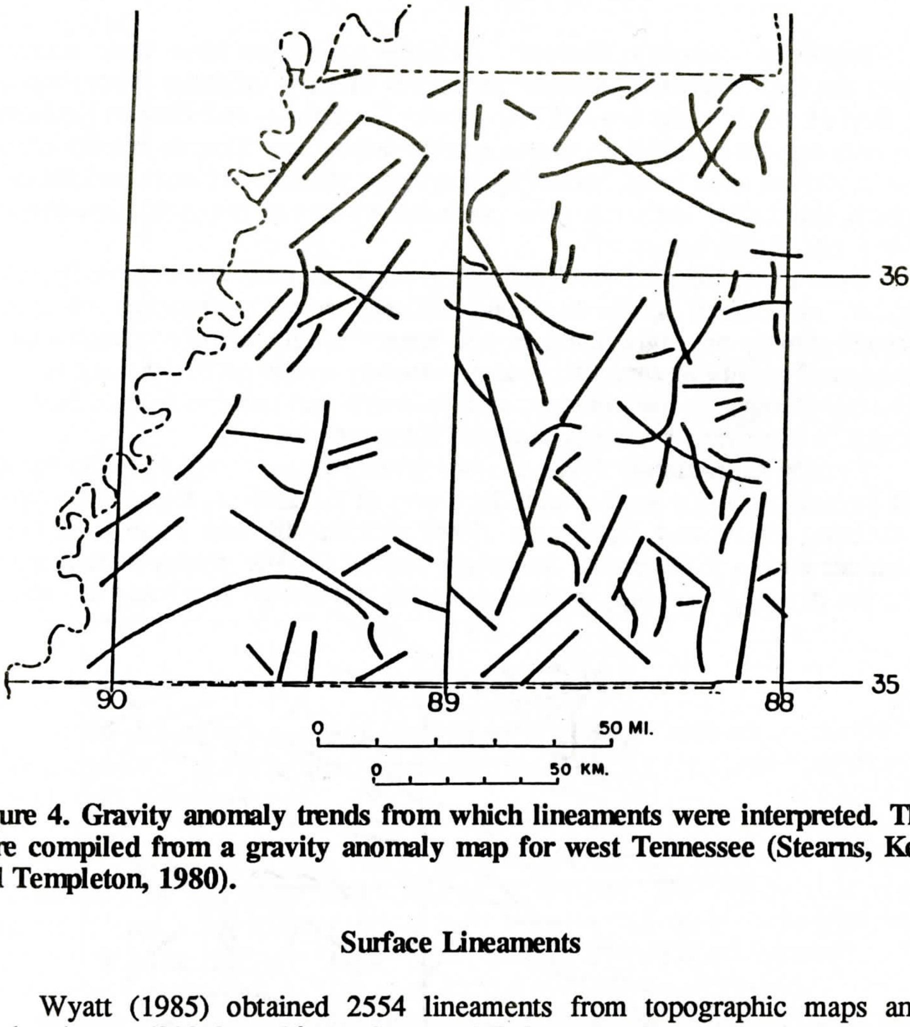

Figure 4. Gravity anomaly trends from which lineaments were interpreted. These were compiled from a gravity anomaly map for west Tennessee (Stearns, Keller and Templeton, 1980).

Surface Lineaments

Wyatt (1985) obtained 2554 lineaments from topographic maps and a Landsat image (239 from 2° AMS map, 550 from Landsat and 1765 from 7 1/2-minute quadrangles). These include: stream segments, a series of alignments of shorter stream segments, drainage highs, escarpments, valleys or valley sides, and changes in tonal patterns or vegetation. The minimum length of a lineament that we recorded from Landsat or AMS Quadrangles was 1.5 miles (2.4 km); the maximum length was 25 miles (40 km). Lineaments as short as 2000 feet (0.4 mi, or 0.24 km) were recorded on the large scale 7 1/2-minute quadrangles. Figure 3 shows the pattern of surface lineaments from Landsat and 2° AMS quadrangles, together with lineaments from 7 1/2-minute quadrangles compiled by Stearns and Wilson (1972).

The Landsat lineaments were compared to manmade features at the same scale on the two AMS maps (Dyersburg NGS 1163, and Blytheville NGS 1162), and if a lineament correlated with a manmade feature, it was dropped from the data. The lineaments from 7 1/2-minute quadrangles were compiled by randomly selecting one of the 7 1/2-minute quadrangles in each 15-minute quadrangle and using that 7 1/2-minute quadrangle as a representative for the 15-minute area.

Gravity and Magnetic Lineaments

Depth to Anomaly Sources: Gravity anomalies have their sources at various depths, whereas magnetic anomalies mostly originate from basement. Variation of depth to the base of low density Cretaceous and Eocene Embayment fill commonly causes shallow-source gravity anomalies. Deeper density contrasts occur in deeper rock units, including Paleozoic sedimentary rock and basement. Magnetic anomalies are commonly produced by lateral magnetization variations within Precambrian basement.

Lineaments derived from anomaly maps include approximately straight magnetic or gravity gradients, approximately straight segments of axes of elongated gravity or magnetic highs, and approximately straight segments of axes of elongated gravity or magnetic lows. Anomaly trends probably mark structures and lateral changes in rock masses; and, although particular rock mass boundaries need not be separated by faults, many of them may be.

Gravity Lineaments: There are two gravity maps; a regional map for all of West Tennessee, and a detailed map for a part of the area. A regional gravity map by Stearns, Keller and Templeton (1980, 1:250,000) was used to obtain the lineaments shown in Figure 4. Its sparse control (3-mile gravity station spacing) limits the detail of the map, so lineaments are relatively few (only 81) and long

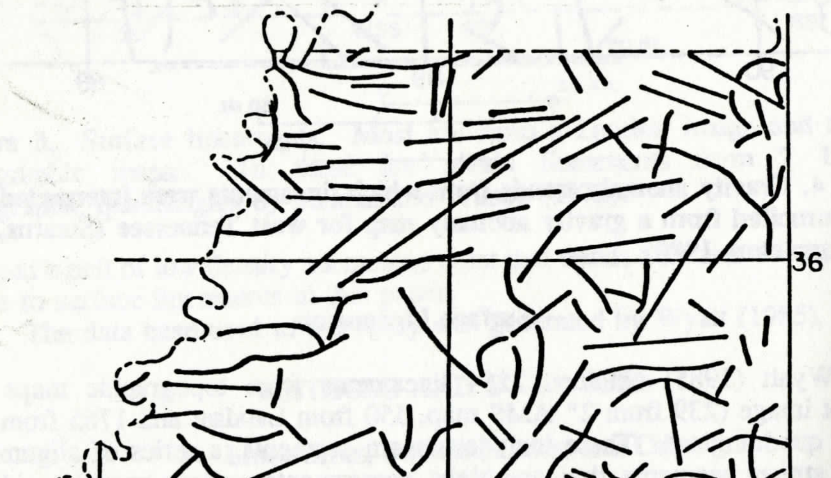

Figure 5. Magnetic anomaly trends from which lineaments were interpreted. These were compiled from the west Tennessee sheet of the Residual Total Aeromagnetic Intensity Map of Johnson and others (1979).

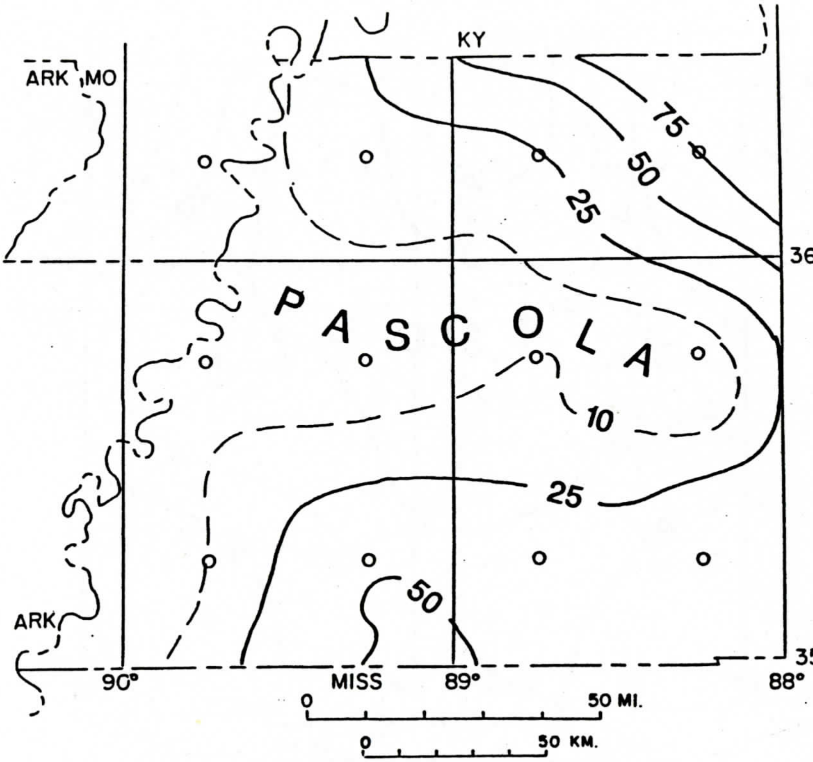

Figure 6. The pattern of frequency of surface lineaments. Contours are numbers of lineaments per 7 1/2-minute quadrangle. The small circles are control points at the center of each 30-minute cell.

(longer than 7 miles or 11 km). More detailed gravity surveys were made in the northwest part of the study area (Stearns, 1980, and also unpublished maps). These maps have a one mile or closer station spacing, so more (110) and shorter lineaments could be delineated in less than half the area of West Tennessee. This more detailed gravity data will be used for the comparisons on Table 1.

Aeromagnetic Lineaments: Aeromagnetic lineaments (Figure 5) were drawn from anomalies on the West Tennessee sheet of the Aeromagnetic Map of Tennessee by Johnson and others (1978). Because of the one mile spacing of flight lines, this map has sufficient detail to draw more than twice as many lineaments (200) than the 81 compiled from the regional gravity map. The one-mile spacing between flight lines is similar to the one-mile spacing of stations for the detailed gravity maps.

VARIATION IN FREQUENCY AND LENGTH OF LINEAMENTS

Maps of the Frequency of Lineaments

Frequency is the number of lineaments in a cell without regard to length. Frequency contour maps are generated by totaling the number of lineaments in a cell and assigning this value to its center (Levandowski and others, 1976)

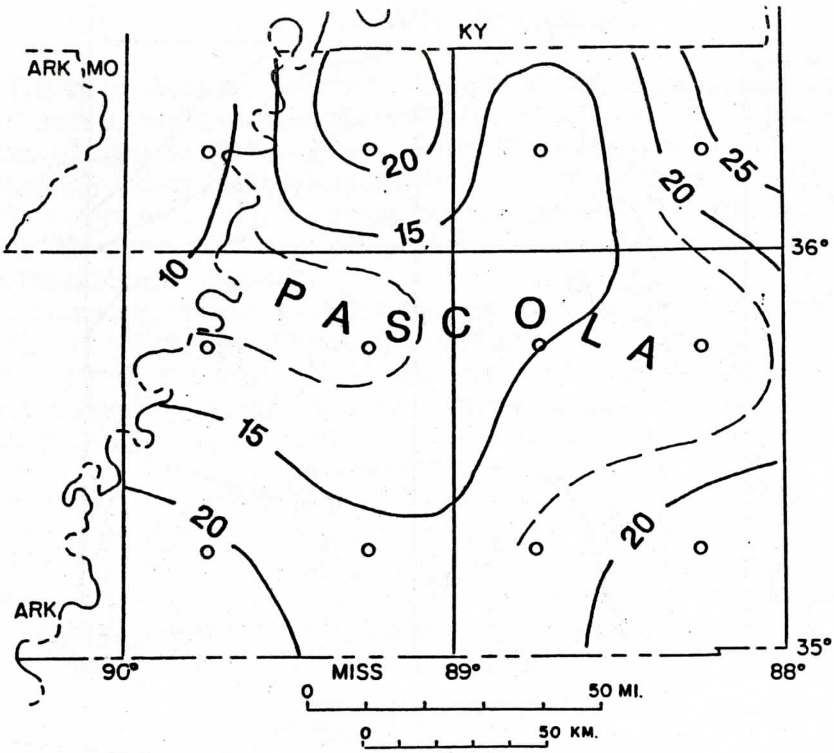

Figure 7. The pattern of frequency of aeromagnetic lineaments. Contours are the number of lineaments per 30-minute cell. The label "PASCOLA" is positioned as on Figure 6 to show that the pattern for these deep source lineaments is comparable to that of surface lineaments.

which becomes a control point for a contour map. The surface lineament frequency map (Figure 6) is based on the 1765 lineaments from the 7 1/2-minute quadrangles, and the magnetic lineament frequency map (Figure 7) is based on the 200 magnetic lineaments. Surface frequency (Figure 6) shows an ESE-trending area of few lineaments (only 2 to 5 per 7 1/2-minute Quadrangle) passing just south of latitude 36N. This trend is roughly coincident with the Pascola arch, a buried post- Pennsylvanian and pre-Cretaceous arch that trends ESE (Schwalb, 1982). For aeromagnetic lineaments (Fig. 7) the frequency pattern is nearly similar; there is an additional low frequency belt that trends SSE. This low that trends SSE from the "PA" in "PASCOLA" to 89° longitude at the south border of Tennessee is similar in trend to Hildenbrand's "low density zone" in the crust (1985, Fig. 6). The partial correlation between surface lineaments and magnetic deeper-seated features associated with the Pascola arch indicates that the surface lineaments are related to pre-Cretaceous and older structures.

Maps of the length of lineaments

Figures 8 and 9 show variations in the lengths of lineaments within cells from the Landsat image and from the magnetic anomaly map. Both show lengths

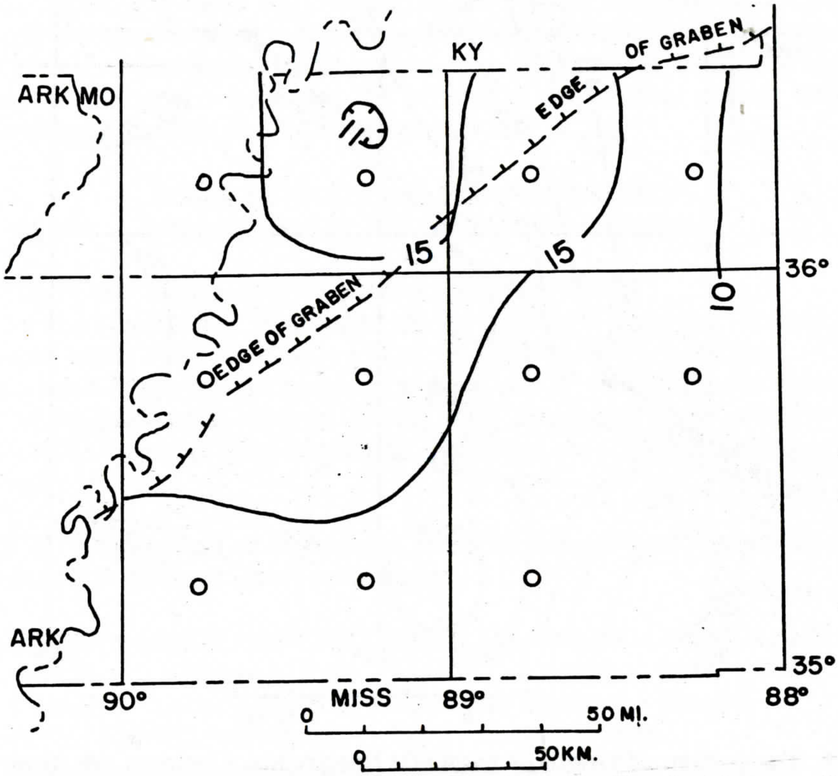

Figure 8. The pattern of length of lineaments from the Landsat image. Contours are mean lengths in miles within each 30-minute cell. The graben edge is from Figure 1.

greater than 10 miles (16 km) over most of the area. Magnetic lineaments originate from the basement, and surface lineaments greater than 10 miles long may be expected to extend deep (see discussion in Podwysocki, 1974). These maps display an approximate NE trend parallel to the the Mississippi Valley Graben. Surface lineaments are longer along the edge of the graben. This trend is expected for Landsat surface lineaments, because the NE trending Reelfoot Rift is an active earthquake zone with known surface fracture expression. Also expected is a parallelism of the Rift with length trends of magnetic anomalies, because Hildenbrand and others (1982) used magnetic information to draw the graben boundary. Magnetic anomalies are longer inside the graben and shorter outside the graben where magnetic basement is shallower.

VARIATION IN THE AZIMUTH OF LINEAMENTS

General

An area of six 30-minute cells in the NW part of West Tennessee will be used to examine the directional relationships of surface and geophysical lineaments. Detailed gravity maps that provide the most numerous geophysical

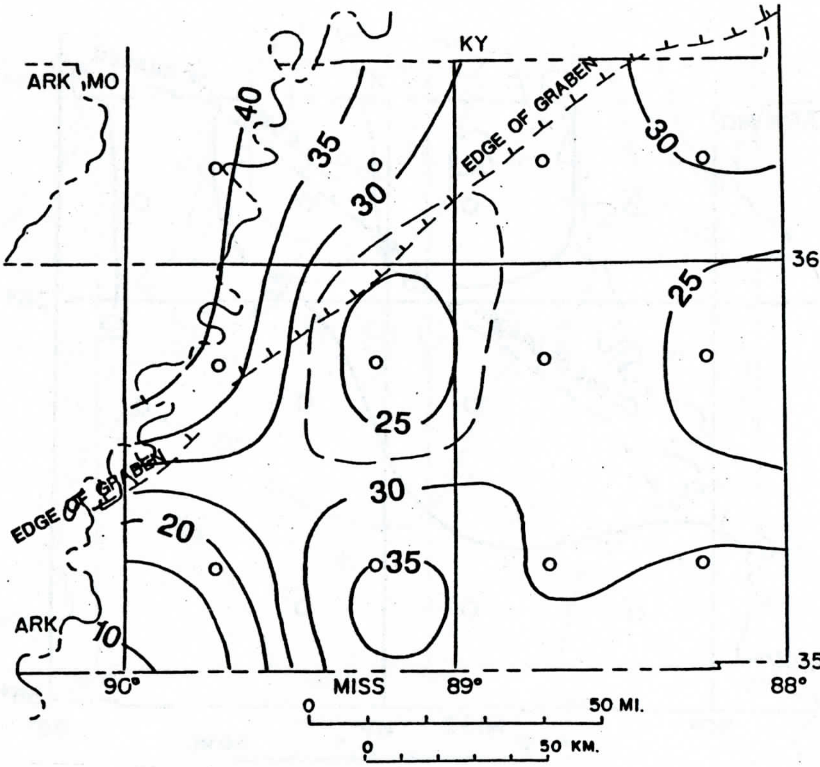

Figure 9. The pattern of length of magnetic lineaments. Contours are mean length in miles within each 30-minute cell.

lineaments in each 30-minute cell are available for this area. This area is also of interest because it contains the edge of the Mississippi Valley graben, and is the site of numerous earthquakes.

Tabulated azimuths of lineaments were combined as classed data in eighteen 10 degree sectors, 0 through 179 degrees. The azimuth data were used in two ways: 1) to compare directions of surface lineaments with the trends of gravity and magnetic anomalies, and 2) to select surface lineaments that are numerous by azimuth class and also parallel to geophysical lineaments. Collective groupings of such selected lineaments form the lineament swarms that are the writers' preferred candidates for fault zones.

Statistical Manipulation

Directions having the most lineaments were emphasized by use of a crude sorting technique analogous to sieving. The sieving procedure is as follows: count the number of lineaments within each 10-degree azimuth sector of each cell, and consider the lineaments falling in the nine (of 18) least populous, azimuth sectors to be a "background noise". Only half of the sectors can survive this process, the rest "falling through" the "sieve". Fewer than half commonly survive, because zero is not an acceptable number for the background. If 9 or more sectors have no lineaments within a cell, then sectors containing only one lineament were also rejected. In several cases this resulted in no sectors surviving in a cell where lineaments are sparse. Such a harsh rejection of lineaments in so many sectors by such a simple technique probably means that many actual fracture traces were rejected, but the writers hope that the benefit of emphasis of sectors having the more numerous lineaments will outweigh this loss.

Results of Sieving and Comparisons Between Surviving Surface and Geophysical Lineaments

The results (Table 1) can be summarized as follows:

1 - In a 30-minute x 30-minute cell, if a ten degree sector has enough surface lineaments, either from Landsat, or AMS or 7 1/2-minute quadrangles, to survive the sieve (each sector has 3 chances to survive, and 67 of 108 sectors did survive), there is about a 63 percent chance that the same ten-degree sector contains enough gravity and/or magnetic lineaments with directional correspondence to survive the sieve also.

TABLE 1. Comparison of occurrence of surface lineaments, gravity lineaments and magnetic lineaments on a sector basis

POSSIBLE SURFACE LINEAMENT COMBINATIONS	POSSIBLE GRAVITY AND MAGNETIC COMBINATIONS				
	Neither Grav. nor Magnetic Lineaments.	Gravity Lineaments Only.	Magnetic Lineaments Only	Both Present	Total
All absent	24	11	4	2	41
One is Present	17	12	7	6	42
Two are Present	7	10	1	3	21
All Present	1	3	0	0	4
Total	49	36	12	11	108

POSSIBLE GRAVITY AND MAGNETIC COMBINATIONS	POSSIBLE SURFACE LINEAMENT COMBINATIONS								
	71/2'Q Only	Landsat Only	AMS Only	71/2+ L.	71/2+ AMS	L+ AMS	All three	none	Total
All absent	8	6	3	4	0	3	1	24	49
Gravity Only	6	5	1	6	1	3	3	11	36
Magnetic Only	1	5	1	0	0	1	0	4	12
Both G and M	2	2	2	1	1	1	0	2	11
Total	17	18	7	11	2	8	4	41	108

There are 18 ten-degree sectors in each cell, and there are six cells, a total of 108 sectors.

2 - If a sector has two or three types of surface lineaments surviving, and 25 of the 67 did, the chance of correspondence with surviving gravity or magnetic

lineaments increases slightly to 68 percent.

3 - If no surface lineaments in a ten degree sector survive the sieve (and 41 of 108 sectors did not survive), there is about a 68 percent chance that in these 41 sectors no gravity or magnetic lineaments survived either.

4 - There is a stronger directional correspondence between surface lineaments and gravity lineaments than with magnetic lineaments. For the 42 sectors having both surviving surface lineaments and surviving gravity or magnetic lineaments, 25 correspond with gravity lineaments only, but only 8 correspond with magnetic lineaments only. This seems predictable for two reasons. In the 6 cell area, there are more than twice as many gravity lineaments (185) than magnetic lineaments (91), so chance could result in a greater correspondence. Also, many gravity anomalies originate closer to the land surface, so proximity to the land surface makes correspondence with the surface more likely.

The most prominent directions of surviving lineaments (not tabulated herein) is four sectors to the NE (30-69°) and three sectors to the SE (130-159°). The direction NE (30-69°) is roughly parallel to the edge of the Mississippi Valley graben (N50E), and therefore is expected, although its dispersion is greater than might be expected from the nearly straight trend drawn by Hildenbrand and others in 1982 (see Figure 1). Argialas (1979) reported this NE direction as 30-60° for Landsat lineaments. The SE (130-159°) direction is apparent on Figures 1-3. It is a previously emphasized direction: Fisk mapped it at about 130° in 1944, and Hildenbrand (1985) mapped a "low density zone" in basement trending about 160°.

MAPS OF LINEAMENT SWARMS

General

First, swarms are drawn using all surface lineaments. Next, swarms are drawn using only those lineaments that both survived the sieve and also are parallel with gravity or magnetic lineaments. The writers consider swarms parallel to geophysical anomalies to be more meaningful; but as will be shown, most swarms appear on both maps.

Lineament Swarms Drawn From Unselected Surface Lineaments

Figure 10 shows about 20 swarms made from all of the lineaments on Figure 3. A swarm must have lineaments that are nearly parallel and nearly end-to-end or closely en-echelon and must collectively be at least 20 miles long. In places, end-to-end selection results in curving swarms; these occur north of 36° and east of 89°. Most of the swarms on this map will reoccur on Figure 12.

Lineament Swarms Drawn From Selected Surface Lineaments

Figure 11 has that portion of the lineaments from Figure 3 that survived the two-stage rejection process; first sieving and then a test of correspondence in

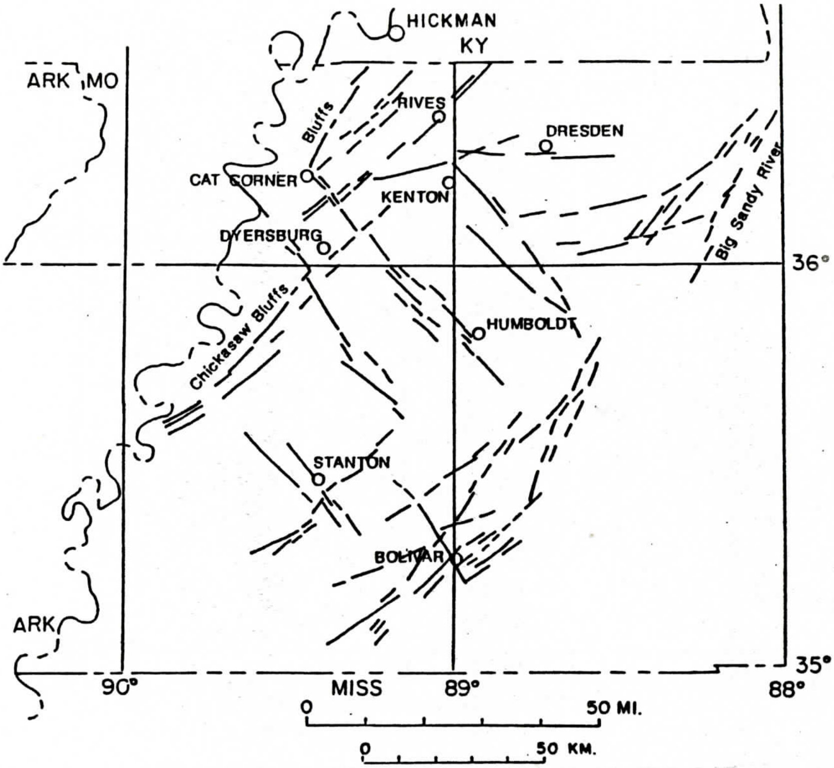

Figure 10. Swarms of lineaments from Figure 3 that collectively are at least 20 miles (32 km) long. The source lineaments are not preselected and are not necessarily parallell to geophysical anomalies.

direction with gravity or magnetic lineaments in the same cell. Outside of the study area of six 30-minute cells, lineaments were tabulated by combining them into larger 45-minute cells. The use of the larger cell size allowed a comparison of surface lineaments with the sparser lineaments from the regional gravity map. If a 30-minute cell had been used, nearly all of the gravity lineaments would have been rejected by sieving, so in turn many surface lineaments would have been rejected as not parallel to surviving geophysical anomaly lineaments. Because many lineaments within about 20° of N-S and E-W are rejected, the NE and SE trending lineament swarms are easy to see on Figure 11.

Figure 12 uses the selected lineaments on Figure 11. To be part of a swarm on this map, the lineaments must be nearly parallel and end-to-end or closely en-echelon, and make an aggregate at least 20 miles (32 km) long. If the two-step selection process is worthwhile, Figure 12 is a more significant map of swarms than Figure 10, but nearly all the swarms on Figure 12 are prominent and clearly expressed on Figure 10, too.

Comparison of the Swarms With Rivers and the Chickasaw Bluffs

It stands to reason that there is coincidence between lineaments and streams,

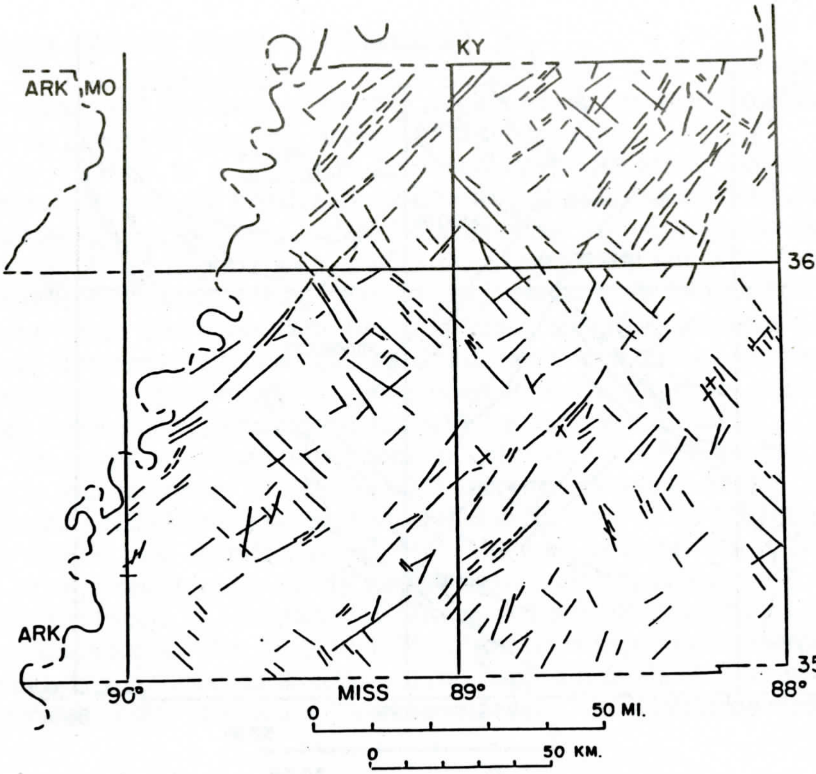

Figure 11. Preselected lineaments. These first survived the sieve and then survived the test of being parallel to gravity or magnetic anomalies.

because many lineaments are defined by straight reaches of streams. It also stands to reason that the largest streams (rivers) would likely coincide with lineament swarms. The SE-trending swarm west of Dyersburg (Dyersburg line) follows the South Fork of Forked Deer River for about 10 miles near the edge of the graben (see Figure 1). The swarm near Kenton mostly follows the Rutherford Fork of the Obion River. The longest swarm from Humboldt to Cat Corner (Humboldt line) partially follows the Middle Fork of Forked Deer River. The swarms in the northeast corner of Figures 10 and 12 coincide with the Big Sandy River and its West Sandy tributary. Some swarms follow lesser streams. The NE-trending swarm through Rives (Rives line) or the one through Bolivar, and the SE-trending swarm through Stanton all follow lesser streams.

Cat Corner marks a prominent right-angle turn in Chickasaw Bluff. Three swarms converge here (Figs. 10, 12). From Cat Corner the NNE-trending swarm ("Hickman fault zone") follows the Bluff into Kentucky along faults mapped by Moore (1965) and Finch (1971). A long straight part of Chickasaw Bluff (part of the Bluff line) expresses the NE-trending swarm southwest of Dyersburg.

Comparisons of Swarms With Earthquakes and Structure

Earthquakes: Earthquakes are deep-seated and sporadic in distribution, so

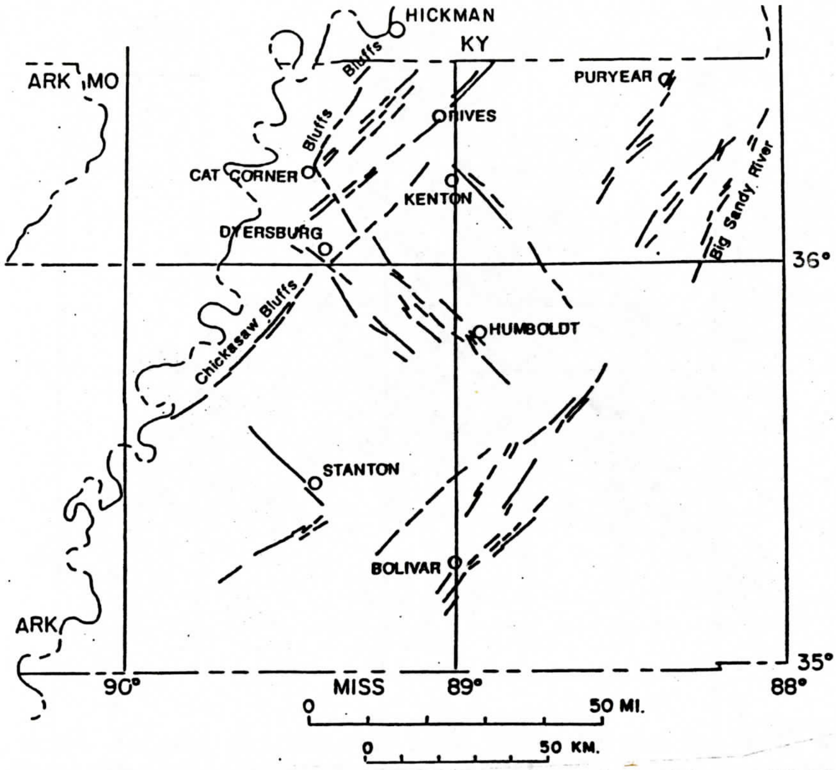

Figure 12. Swarms of the preselected lineaments from Figure 11 that are collectively at least 20 miles (32 km) long.

the location of any earthquake near a surface lineament could be pure coincidence. Nevertheless, an earthquake near any swarm is a possible indication that the swarm is a surface expression of an active fault zone. Figure 13 shows the swarms near earthquake epicenters located by seismograph nets of the St. Louis University and the Tennessee Earthquake Information Center. One important relationship based on many earthquakes is the shift in epicenters of earthquake swarms (stipples) across the Mississippi River along the SE-trending Dyersburg line. Southwest of this line most earthquakes are in a narrow belt in Missouri and Arkansas. Northeast of this line earthquakes shift across the Mississippi River into a broad band in Tennessee. It is interesting that one earthquake coincides with the southeast end of the Dyersburg line, and that the longest SE-trending swarm (the Humboldt line), which extends from Cat Corner near the Mississippi River to Humboldt, has three isolated earthquakes near Humboldt.

Faults: Only one swarm (Rives line) has a fault observed at the land surface. A fault (Figure 13) along the Rives line was mapped in the Water Valley quadrangle in Kentucky by Finch (1963). This fault is about 9 miles (14 km) from the Tennessee border. Its strike is parallel to the swarm and it occurs in a stream valley that is a continuation of the Tennessee part.

Only one swarm (Hickman fault zone) has faults mapped over most of its length; this is the Chickasaw Bluff near the Tennessee-Kentucky border. Moore (1965) mapped a post-Eocene and pre-Holocene buried fault in Tennessee using

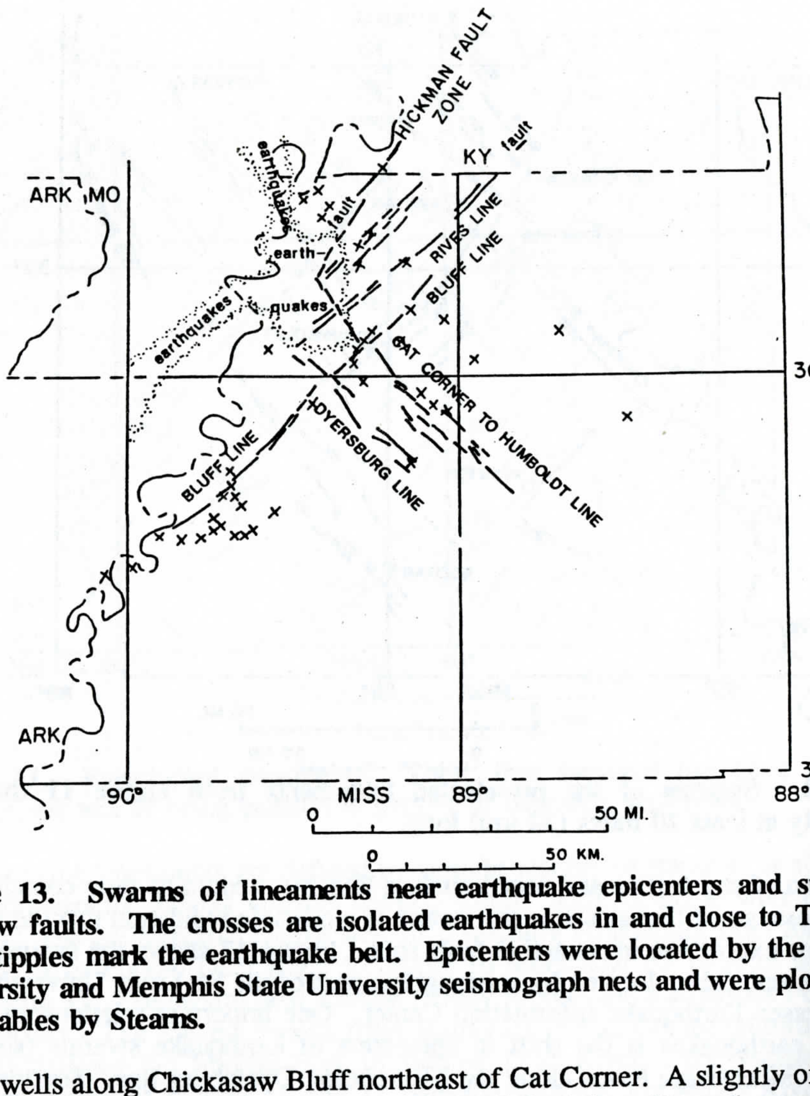

Figure 13. Swarms of lineaments near earthquake epicenters and surface or shallow faults. The crosses are isolated earthquakes in and close to Tennessee. The stipples mark the earthquake belt. Epicenters were located by the St. Louis University and Memphis State University seismograph nets and were plotted from their tables by Stearns.

water wells along Chickasaw Bluff northeast of Cat Corner. A slightly offset fault was mapped along the bluff about 5 miles (8 km) into Kentucky to Hickman (Finch, 1971, and McDowell and others, 1981). Like the one in Tennessee, this fault is buried by Mississippi River alluvium.

Subsurface Structure: The top of magnetic basement as drawn by Stearns and Reesman (1986) has a prominent SE-trending low that coincides with the 55-mile long (88 km) Humboldt line (Figure 14). This basement low could be a graben connecting with the Mississippi Valley graben, and the Humboldt line could be surface faults over a reactivated graben.

Comparison of the Swarms with Lineaments Drawn by Fisk in 1944

Fisk drew eight lineaments in our 6 cell study area (Figure 2). Each is

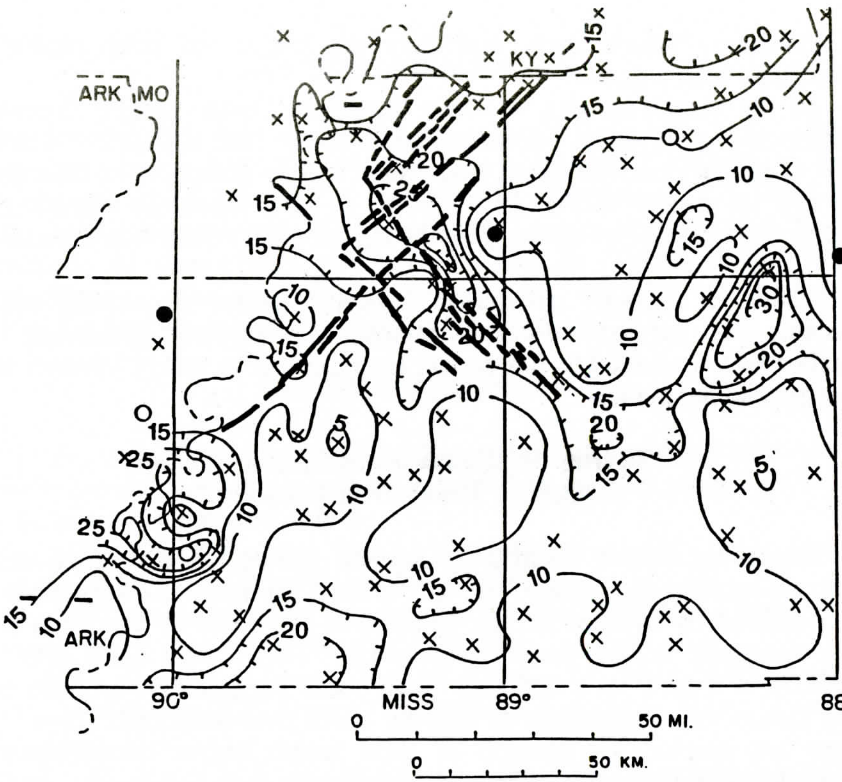

Figure 14. Swarms of lineaments from Figure 13 and the depth to magneti basement (from Stearns and Reesman, 1986). Contours are thousands of fee below sea level. Note the coincidence between the longest SE-trending Humbold Line and the 10-to 15 thousand-foot SE-trending low on magnetic basement.

about 30 or more miles (48 km) long and they trend parallel to swarms defined b this study. His map was at a very small scale, so precise agreement is not to be expected. He refers to his line segments as "generalized position of fault zone" Where Fisk mapped two NE-trending lineaments of the Big Creek fault zone w map four swarms. The faults mapped by Moore (1965) and Finch (1971) partiall verify Fisk's interpretation that the NE-trending lineaments near Chickasaw Bluf are faults. The NE-trending swarms of this report could be a more detailed map o the Big Creek fault zone. The two longest SE-trending swarms of this report d not agree in location with those drawn by Fisk, but they do coincide in directio (compare Figures 2 and 12).

CONCLUSIONS

Pattern, Direction and Interrelationships of Lineaments

Maps of the frequency and length of surface lineaments from Landsat, and 7 1/2-minute quadrangles are similar in pattern to maps of frequency and length o lineaments from magnetic anomaly maps. Lineaments are fewer over the burie pre-Cretaceous Pascola arch, and they are longer in belts parallel to the Mississipppi Valley graben.

In the northwest part of West Tennessee, most surface lineaments and corresponding geophysical lineaments trend 30-69° and 130-159°. The direction 30-69° is roughly parallel to the Mississippi Valley graben. The direction 130 to about 145° is parallel to the late Paleozoic or early Mesozoic Pascola arch. The direction 159° is parallel to the trend of Hildenbrand's (1985) low density crustal zone.

There is a closer parallelism between surface lineaments and gravity lineaments than between surface lineaments and magnetic lineaments. Gravity anomalies have a shallower source and are more apt to reflect younger structures than magnetic anomalies.

Swarms of Lineaments as Surface Faults or Fracture Traces Over Deep Faults

There are fifteen swarms of surface lineaments that trend end-to-end, closely en-echelon and collectively are at least 20 miles (32 km) long. All are further defined by selected surface lineaments that trend in directions parallel to nearby magnetic and/or gravity anomalies. The writers name five of these informally as a fault zone and four "lines", and suggest that they are concealed young faults or concentrations of fracture traces over deep fault zones. The five swarms are emphasized because of their length and/or correspondence with previously mapped faults or nearby earthquakes.

1- The "Hickman fault zone" extends NE from Cat Corner along Chickasaw Bluff to near Hickman, Kentucky. It is associated with established post-Eocene faults for most of its 35 mile (56 km) length, and is nearly precisely one of the lineaments drawn by Fisk in 1944 as part of his "Big Creek fault zone".

2- The Rives line extends about 55 miles (88 km) NE from near Dyersburg into Kentucky. It has a surface fault at its NE end, and its SW terminus lies within an earthquake swarm.

3- The Bluff line is the longest one mapped herein (about 60 miles or 96 km). It trends NE parallel with the Rives line. For about half of its length it follows Chickasaw Bluff (the edge of the Mississippi River alluvial plain).

4- The Dyersburg line offsets the main New Madrid microearthquake belt. It extends SE about 45 miles (72 km) and terminates near a single earthquake epicenter. The single occurrence could be a mere coincidence, but the offset of the earthquake belt is not.

5- The Humboldt line trends SE for about 50 miles (80 km) from the abrupt corner in the Chickasaw Bluff. It coincides with a low in magnetic basement (possibly a graben).

The writers suggest that the swarms merit continued interest as belts in which to localize and focus investigations. It is possible that they are presently active (maybe reactivated) lengthy faults with some slight or considerable offset in Eocene or even Holocene sediments.

ACKNOWLEDGMENTS

This investigation was supported by a grant from the U.S. Nuclear Regulatory Commission (NRC-04-81-195-02) to Vanderbilt University as part of the New Madrid Study Group, T.C. Buschbach, Coordinator and Dr. Edward O'Donnell, technical supervisor. The manuscript was much improved thanks to Arthur Reesman of Vanderbilt University and Thomas Hildenbrand of the U.S. Geological Survey. The enhanced Landsat image used in this project was furnished by Herbert Tiedemann of Phillips Oil Company.

REFERENCES CITED

Argialas, Demetre P., 1979, Mapping and comparison of Landsat lineaments with gravity trends in West Tennessee: unpublished master's thesis, University of Tennessee, Knoxville, 166 p.

Finch, W.I., 1963, Geology of the Water Valley quadrangle, Ky.: U.S. Geological Survey, Quad. map G.Q. 269, scale 1:24,000.

Finch, W.I., 1971, Geology of the Hickman quadrangle, Ky.: U.S. Geological Survey, Quad. map GQ-874, scale 1:24,000.

Fisk, H.N., 1944, Geological investigation of the alluvial valley of the lower Mississippi River: U.S. Army Corps of Engineers, Miss. River Comm., Vicksburg, Miss., 78 p.

Hildenbrand, T.G., Kane, M.F. and Hendricks, J.D., 1982, Magnetic basement in the Upper Mississippi Embayment Region - A Preliminary Report, Investigations of the New Madrid, Missouri, Earthquake Region: U.S. Geological Survey Professional Paper 1236-E, 38 p.

Hildenbrand, T.G., 1985, Rift structure of the Northern Mississippi Embayment from the analysis of gravity and magnetic data, Jour. of Geophysical Res., Vol. 90, No. B14, p. 12,607-12,622.

Johnson, R.W., Haygood, C. and Kunselman, P.M., 1978, Residual total intensity aeromagnetic map of Tennessee, west sheet: Tennessee Division of Geology, scale 1:250,000.

Levandowski, D.W., Jennings, T.V. and Lehman, T.W., 1976, Relations between ERTS lineaments, aeromagnetic anomalies, and geologic structures in north-central Nevada: in R.A. Hodgson, S.P. Gay, and J.Y. Benjamins, eds., Proceedings of First International Conference on New Basement Tectonics, Publication 5, p. 106-117.

McDowell, R.C., Grabowski, J.G., Jr., and Moore, S.L., 1981, Geologic Map of Kentucky: Ky. Geological Survey and U.S. Geological Survey, Geologic map, scale 1:250,000.

Moore, G.K., 1965, Geology and hydrology of the Claiborne Group in western Tennessee: U.S. Geological Survey, Water Supply Paper 1809-F.

O'Leary, D.W., Friedman, J.D., and Pohn, H.A., 1976, Lineament, linear, lineation: some proposed new standards for old terms, Geol Soc. of Amer, Bull., Vol. 87, p. 1463-1469.

O'Leary, D.W., and Simpson, S.L., 1977, Remote sensing applications to tectonism and seismicity in the northern part of the Mississsippi Embayment: Geophysics, vol. 42. no. 3, p. 542-548.

Podwysocki, M.H., 1974, An analysis of fracture trace patterns in areas of flat-lying sedimentary rocks for the detection of buried geologic structure: Goddard Space Flight Center, CSFC X-923-74-200.

Sabins, F.F., 1978, Remote Sensing, Principals and Interpretations: San Francisco, 426 p.

Schwalb, H.R., 1982, Paleozoic geology of the New Madrid area: U.S. Nuclear Regulatory Commission, NUREG/CR-2909, 61p.

Stearns, R.G., and Wilson, C.W., Jr., 1972, Relationships of earthquakes and geology in West Tennessee and adjacent areas: Tennessee Valley Authority, Knoxville, Tenn., 296 p.

Stearns, R.G., Keller, G.R. and Templeton, T.R., 1980, Gravity anomaly map of Tennessee, west sheet: Tennessee Division of Geology, scale 1:250,000.

Stearns, R.G., 1980, Gravity anomaly map of the Reelfoot Lake area, Tennessee: Tenn. Division of Geology, scale 1:62,500.

Stearns, R.G. and Reesman, A.L., 1986, Cambrian to Holocene structural and burial history of Nashville dome: AAPG Bulletin, v. 70, no. 2, p 143-154.

Tennessee Earthquake Information Center, 1980 to present, Preliminary seismological bulletins: Metzger, A, Nava, S.J. and others, Editors.

Wyatt, D.E., Jr., 1985, Geomorphic, gravity and magnetic lineaments in West Tennessee- implications to location of the east edge of Reelfoot Rift: unpublished master's thesis, Vanderbilt University, Nashville, Tenn., 172 p.

EVIDENCE OF QUATERNARY GROUND TILTING ASSOCIATED WITH THE REELFOOT RIFT ZONE, NORTHEAST ARKANSAS

RANDEL TOM COX *Department of Geology, University of Arkansas Fayetteville, AR 72701*

ABSTRACT

The Mississippi Embayment is underlain by the seismically active Reelfoot Rift zone. Crowley's Ridge is an erosional remnant of Pleistocene incision. Abrupt changes along this ridge in geology, width, bearing, and transverse topographic symmetry suggest that the areas north and south of latitude 35° 45'N have had different Quaternary tectonic histories. Drainage basins interior to Crowley's Ridge show a significant difference in transverse symmetry and bearing north and south of latitude 35° 45'N. These two areas could overlie separate crustal blocks that behave differently. North of latitude 35° 45'N, the orientations of basins exhibiting the greatest asymmetry suggest preferred stream migration in response to S 65° E tilting. This observation is consistent with the hypothesis that E-SE migration of the rivers adjacent to the northern ridge gave rise to the topographic asymmetry of the ridge there. The age of the topography restricts this period of E-SE ground tilting to Quaternary time. Multiple regression analysis of the base of the Plio-Pleistocene deposits capping Crowley's Ridge suggests that the area of the ridge north of latitude 35° 45'N has been down-dropped relative to the area to the south.

At 35° 45'N, a linear segment of the western ridge margin oriented N 61° W could be the exhumed scarp of a fault separating the two blocks. This linear feature is parallel to the direction of proposed tilting and intersects the point of abrupt change in ridge geology and geomorphology. Projection of this lineament approximates the southern end of New Madrid seismicity.

INTRODUCTION

The Mississippi Embayment is underlain by the Reelfoot Rift zone, the most seismically active structural province of the eastern United States (Zoback and others, 1980). The landforms of the Mississippi Embayment in northeast Arkansas include the Mississippi River and St. Francis River basins in the east, the Cache River basin in the west, and Crowley's Ridge dividing these two lowlands (Figure 1). The north-northeast trending Crowley's Ridge is an erosional remnant which reveals the stratigraphy of the Mississippi Embayment prior to Quaternary incision (Call, 1891; Stephenson and Crider, 1916; Fisk, 1944; Guccione and others, 1986). Aspects of the geology and geomorphology of Crowley's Ridge suggest faulting and Quaternary ground tilting and will be the primary subjects of this discussion.

The crest of Crowley's Ridge averages 60 m above the adjacent lowlands. The stratigraphy preserved in the ridge is represented in Figure 2. The Eocene sequence is dominated by unconsolidated continental and deltaic sands and clays

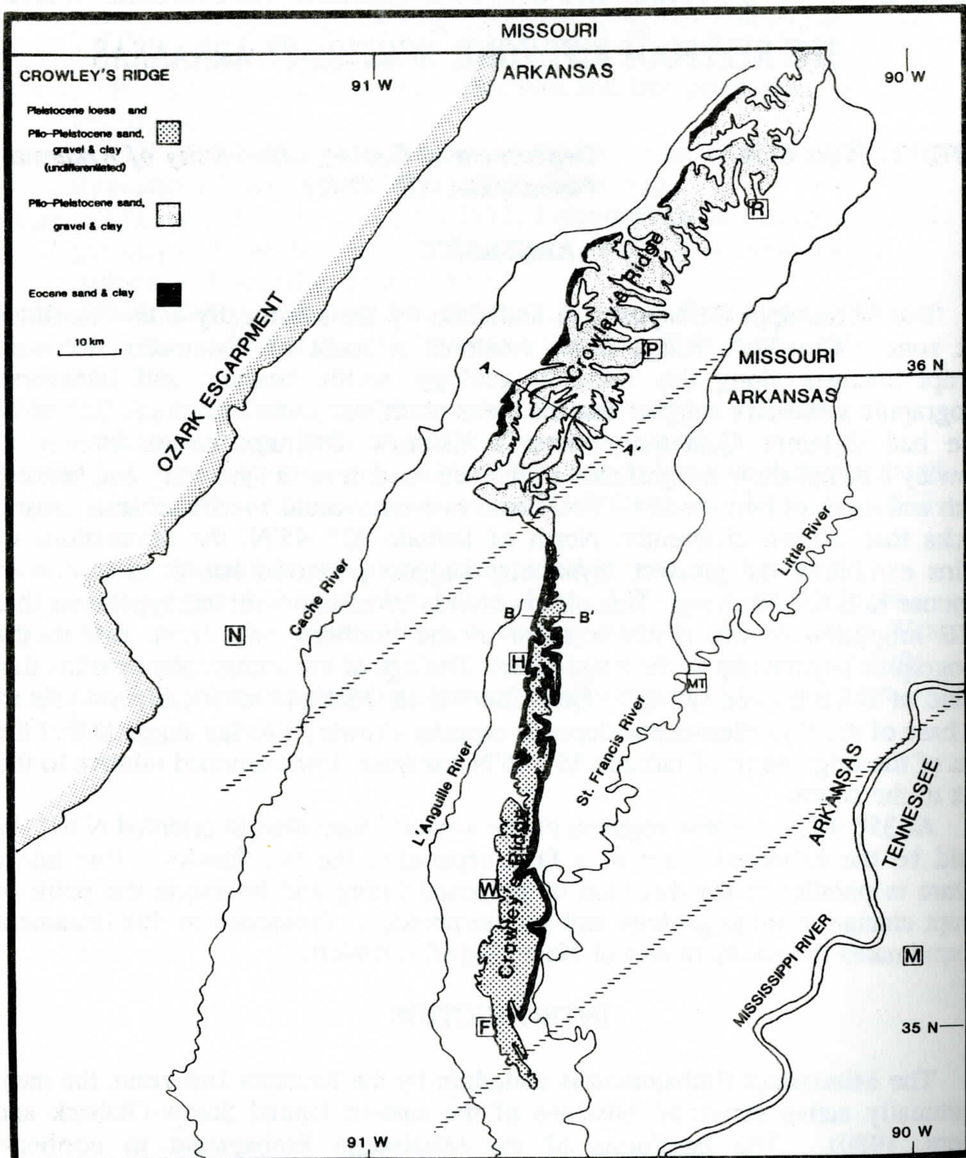

Figure 1. Map of northeastern Arkansas showing major geomorphic features and the geology of Crowley's Ridge (modified after Halley, 1976). Dashed lines represent the margins of the Reelfoot Rift zone (Hilderbrand and others, 1982). Boxes represent towns: R = Rector; P = Paragould; J = Jonesboro; N = Newport; H = Harrisburg; MT = Marked Tree; W = Wynne; M = Memphis; F = Forrest City.

with minor intervals of lignite (Murray, 1961). The Eocene units dip approximately 0.5° SE (Meissner, 1984) and are overlain with angular unconformity by fluvial sands, gravels and clays. In excess of 50 m of these overlying fluvial sediments were encountered in lignite exploration holes drilled on Crowley's Ridge (Holbrook, 1980) (logs on file at the Arkansas Geological Commission). These

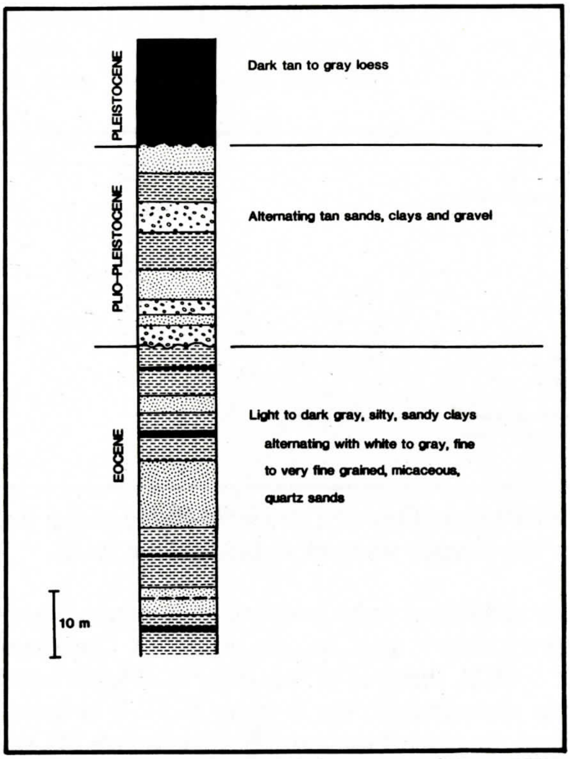

Figure 2. Generalized stratigraphic column for Crowley's Ridge compiled from surface investigations, surface descriptions (Call, 1889; Fisk, 1944; Saucier, 1974; Guccione and others, 1986), and subsurface descriptions (Holbrook, 1980).

Pliocene and/or Pleistocene fluvial deposits are possibly time equivalents of the Lafayette gravel and Citronelle Formation of the Gulf Coast (Potter, 1955; Saucier, 1974; Guccione and others, 1986). Above these fluvial deposits, up to 30 m of Pleistocene loess is locally preserved (Saucier, 1974). Major loess accumulations are confined to the southern portion of Crowley's Ridge (Guccione and others, 1986) (Figure 1).

At latitude 35° 45'N, Crowley's Ridge abruptly changes width, geology, bearing, and transverse topographic symmetry. The ridge north and south of the change shows little transition in these characters. These two areas of Crowley's Ridge will be hereafter referred to as the northern ridge and the southern ridge.

The differences in width and geology between the northern and southern ridges may be related. The northern ridge is wide; it averages 14.5 km, whereas the southern ridge averages 6.5 km (Figure 1). Eocene sands and clays are only locally exposed along the western margin of the northern ridge and Plio-Pleistocene fluvial sands, gravels and clays are exposed throughout the rest of the northern ridge. In contrast, unconsolidated Eocene sediments are widely exposed on both flanks of the southern ridge (Figure 1). If the gravel bearing Plio-Pleistocene deposits offer greater resistance to erosion than the Eocene sands and clays, the difference in the geology of the northern and southern ridges may have allowed more rapid erosion of the southern ridge by laterally corrading streams.

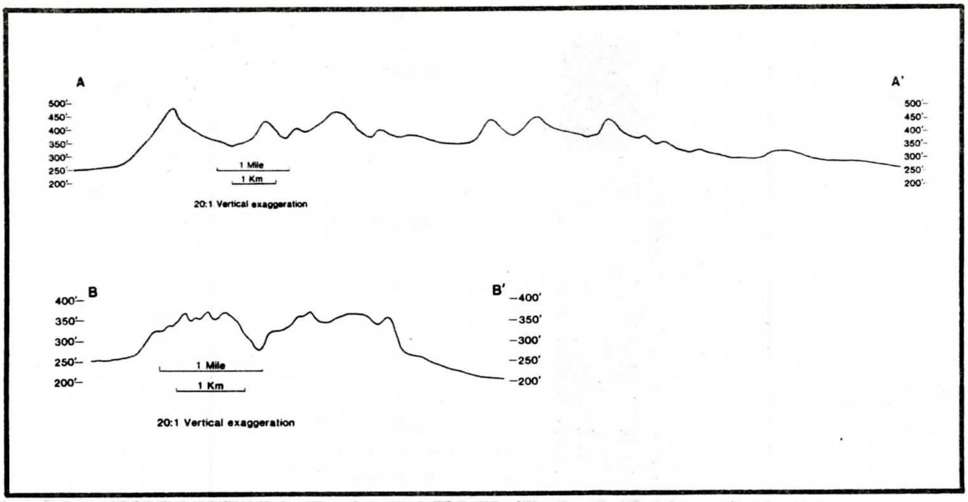

Figure 3. Transverse profiles of Crowley's Ridge along lines A-A' and B-B' on Figure 1. Notice the steeper western slopes on line A-A'.

The differences in bearing and transverse topographic symmetry between the northern and southern ridges may be the result of Quaternary ground tilting. North of latitude 35° 45'N, the axis of the ridge is straight bearing N 30° E. To the south, the axis is also straight, but it bears N 5° E (Figure 1). The northern ridge is asymmetrical in transverse profile relative to the southern ridge, the northern ridge being steeper on the west (Figure 3). The change in transverse symmetry is abrupt at latitude 35° 45'N.

Assuming that the steepness of slope along the margins of the northern and southern ridges in large part reflects the recency of stream erosion along those margins, the pronounced asymmetry of the northern ridge suggests a period of preferred east-southeast migration of the adjacent streams. The rivers adjacent to the northern ridge, the St. Francis and the Cache (Figure 1), are alluvial streams as opposed to bedrock streams. Preferred migration in alluvial streams can be attributed to minute changes in regional slope (Adams, 1980; Schumm, 1986). Thus, the evidence of preferred stream migration in the vicinity of the northern ridge suggests a period of east-southeast ground tilting there. As the Cache River is now located some distance from the western slope of the northern ridge, this period of tilting has apparently ended. The Pleistocene age of Crowley's Ridge as a topographic feature (Saucier, 1974; Guccione and others, 1986) restricts the timing of the end of this period of tilting to the Quaternary.

Adams (1980) suggests that slow oscillations of deep seated crustal blocks are producing oscillating ground tilting in the Mississippi Valley region. The point of change in bearing and transverse symmetry along Crowley's Ridge at latitude 35° 45'N may mark the position of a boundary between such oscillating blocks. As this point of change is located directly above the Jonesboro Pluton (Figure 4), it is reasonable to suggest that this point overlies a zone of weakness in the basement. Mooney and others (1983) report that seismic and gravity data define an anomalously thick area of lower crust underlying a portion of the northeast trending Reelfoot Rift zone. This anomalous layer thins gradually beyond the margins of the rift zone but thins sharply to the southwest along a trend that coincides with the point of change in Crowley's Ridge. The southwestern limit of the thickened lower crust may mark the boundary of a crustal block.

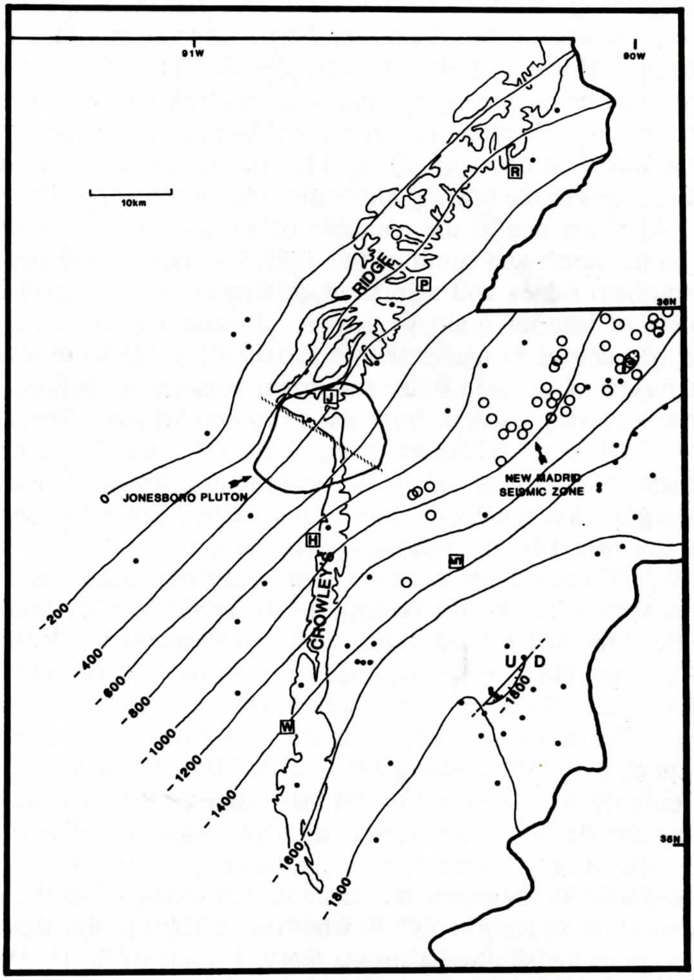

Figure 4. Map showing structural contours (in feet subsea) on the base of the Eocene, and showing spatial relationships of Crowley's Ridge, the New Madrid seismic zone, and the Jonesboro pluton (after Hildenbrand and others, 1982). Dots are drill hole locations. The dashed line represents the proposed fault trend. Earthquake epicenters (open circles) are from Stauder and others (1979). Boxes represent towns: R = Rector; P = Paragould; J = Jonesboro; H = Harrisburg; MT = Marked Tree; W = Wynne.

The above discussion suggests that the areas of Crowley's Ridge north and south of latitude 35° 45'N overlie separate structural blocks which have experienced relative motion during Quaternary time. The objective of this paper is to test this hypothesis using both geomorphic and subsurface evidence.

METHODS AND RESULTS

Analysis of Interior Basin Symmetry

Cross-valley tilt gives rise to preferred lateral stream migration (Price and Whetstone, 1977; Adams, 1980; Schumm, 1986), and down-valley tilt increases headward erosion (Horton, 1945; Parker, 1977). Therefore, the transverse topographic symmetries of drainage basins will be altered by lateral migration of the principal stream in the direction of tilting and by increased headward erosion of tributaries in the direction opposite tilting. The hypothesis developed above states that the abrupt changes in the bearing and transverse symmetry of Crowley's Ridge at latitude 35° 45'N are due to the response of the adjacent rivers to differential ground tilting to the north and south of this latitude. This hypothesis predicts the northern and southern ridges will also show differences with respect to the transverse symmetries of interior drainage basins. To test the hypothesis using this prediction, the symmetries of basins within Crowley's Ridge were investigated.

Drainage basins of all third order and larger streams (as defined by Strahler, 1952) interior to Crowley's Ridge from the Missouri-Arkansas border southward to latitude 34° 52'N were delineated using 1:24,000 scale 7.5 minute U.S.G.S. topographic maps. The alluvial valley of the principal stream of each basin was divided into straight 1 km segments. For each straight 1 km valley segment, basin symmetry was quantified by the following procedure.

The bearing of each 1 km segment was recorded. Then, as a measure of transverse basin symmetry (T), the position of the alluvial valley mid-line relative to the basin mid-line was recorded for each 1 km segment. The value T was expressed as the ratio Da/Dd (Da = the distance from the alluvial valley mid-line to the basin mid-line, and Dd = the distance from the basin divide to the basin mid-line)(Figure 5). The alluvial valley mid-line was assumed to approximate the average position of the stream during the alluvial history of the valley. Drainage divides were defined as the boundary of that area drained by all lower order streams entering the stream of the valley segment under consideration. T values were assigned a direction perpendicular to the bearing of the 1 km valley segment denoting which divide the segment was nearest. For example, in Figure 5 a 1 km alluvial valley segment bearing N 58° W which is 31/100's of the distance from the center of the basin to the southwest divide has a T value of 0.31° SW.

For evaluation of interior drainage basin symmetry, the study area was divided at latitude 35° 45'N. Bearing/T observations of all 1 km alluvial valley segments of third order and larger streams were statistically analyzed to determine if the two sub-areas show significant differences. Three hundred observations were recorded (Figure 6). Basins of first and second order streams show markedly less asymmetry and were not included in the analysis. Stating the null hypothesis (Ho) as "Transverse symmetry (T) and alluvial valley bearing are independent of geographic location (northern or southern ridge)" and the alternate hypothesis (Hi) as "Transverse symmetry and alluvial valley bearing have some dependency on geographic location", the Pearson Chi-square test was employed at 0.01 significance. The corresponding probability value was 0.000 and therefore Ho was rejected. Thus, the Bearing/T distributions of valley segments of the northern and southern ridges show significant differences, and this is interpreted as evidence

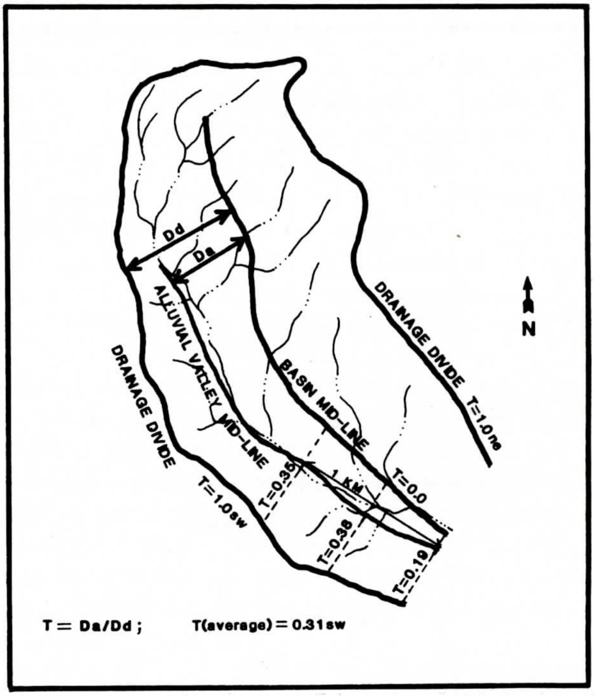

Figure 5. Example of the method used to calculate transverse topographic symmetry (T) for straight 1 km alluvial valley segments. The alluvial valley mid-line is assumed to approximate the average position of the stream during the alluvial history of the valley. The bearing of the first straight 1 km segment for this basin is N 58° W. Position of the alluvial valley mid-line (T) was expressed as the ratio Da/Dd (Da = the distance from the alluvial valley mid-line to the basin mid-line, and Dd = the distance from the basin divide to the basin mid-line). T values were measured at each end and at the middle of the 1 km segment and averaged. The bearing/T value for this 1 km segment is N 58° W/0.31° SW.

that these two areas of Crowley's Ridge overlie separate crustal blocks which have behaved differently during development of the present topography.

For basins exhibiting preferred transverse asymmetry, alluvial valleys are assumed to be shifted from the center of the basin by enhanced stream migration in a direction normal to the strike of bedding or of a tilting block. Basins oriented normal to the direction of such enhanced stream migration will exhibit the greatest asymmetry. On the northern ridge, the valley segments bearing N 20-30° E show the greatest preferred basin asymmetry (Figure 6) suggesting a S 60-70° E direction of enhanced stream migration. It does not seem likely that the existing southeast dip of the Eocene sediments is contributing to preferred stream migration because (a) the Eocene sands and clays are unconsolidated, (b) the 0.5° SE dip of the Eocene units is the same for both the northern and southern ridges and (c) the majority of the basins that suggest east-southeast migration are floored in Plio-Pleistocene sediments overlying the dipping Eocene units. Thus, a period of S 60-70° E tilting is interpreted as having produced the preferred migration. The present non-preferred position of streams in their flood plains suggests that this

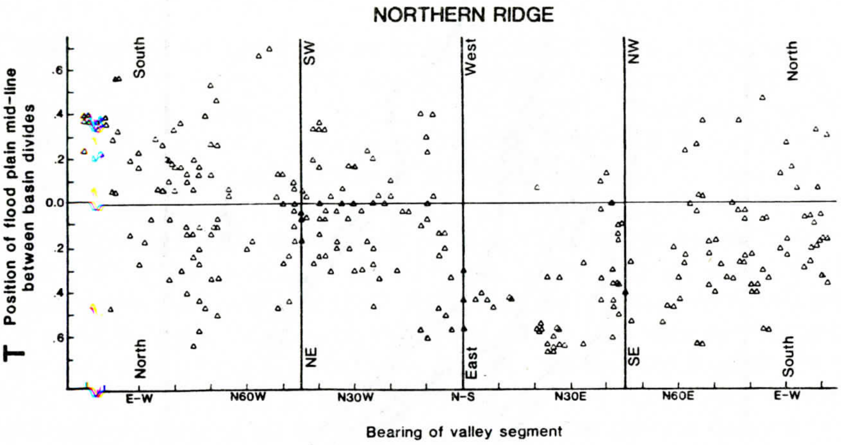

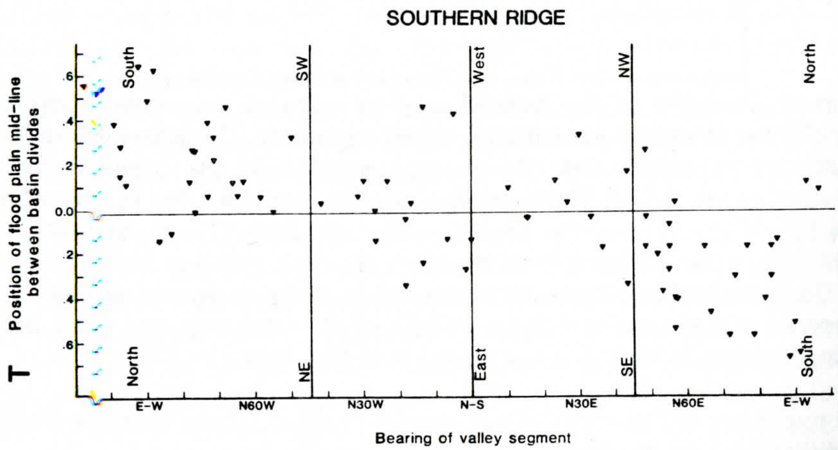

PEARSON CHI SQUARE TEST

Ho: Symmetry and bearing of valley segments are independent of geographic location (northern or southern ridge).

Hi: Symmetry and bearing of valley segments have some dependency on geographic location.

Test statistic = 28.518 (having a Chi-sq distribution with 7 DF under Ho).
Significance level = 0.01; probability value = 0.000.

Figure 6. Transverse symmetry (T) values plotted against bearing for each of 300 one km alluvial valley segments interior to Crowley's Ridge. Greater T values denote greater basin asymmetry. The data were divided into "northern ridge" and "southern ridge" sets at latitude 35° 45'N.

period of east-southeast migration has ended.

On the southern ridge, basin geometries are different. There is a preferred stream migration in a general southerly direction (Figure 6). As this direction is close to the bearing of the southern ridge and adjacent rivers (possibly reflecting the down-slope direction on the pre-dissection surface), the transverse symmetry of the southern ridge has not been influenced. It is interesting that the most common valley segment orientation on the southern ridge is N 45-55° E, a direction parallel to the trend of the underlying Reelfoot Rift (Figure 1).

Analysis of Displacement Between the Northern and Southern Ridges

The hypothesis that the northern and southern ridges overlie separate structural blocks predicts a fault near latitude 35° 45'N on the ridge. Subsurface data from petroleum exploration wells in the region are sparse, but lignite exploration drill holes on Crowley's Ridge (Holbrook, 1980) (logs on file at the Arkansas Geological Commission) provide relatively dense well control in the vicinity of the proposed fault. The basal unconformity of the Plio-Pleistocene interval is the only horizon that can be traced across latitude 35° 45'N in the logs of these shallow exploration holes, so this horizon was examined for possible vertical displacement at latitude 35° 45'N.

As much as 40 m of local relief on the basal Plio-Pleistocene unconformity complicates identification of fault displacement. In order to test for vertical displacement between the northern and southern ridges, best fit planes for the unconformity were calculated by multiple regression analysis using elevations from the lignite exploration holes (Holbrook, 1980). Only logs from holes drilled on highest surfaces of the ridge were used in determining the elevation of the unconformity in order to avoid confusion of the Plio-Pleistocene fluvial deposits with lower, younger Pleistocene terrace deposits or with unsuspected landslides.

A 120 km length of the ridge within 60 km north and south of latitude 35° 45'N was investigated (Figure 7). One hundred and four elevations of the base of the Plio-Pleistocene interval were used in multiple regression analysis (59 from the northern ridge and 45 from the southern ridge). A model plane for the entire 120 km study area was compared to model planes for contiguous 60 km lengths of the northern and southern ridges. The single plane (unfaulted) model was compared to the dual plane (faulted) model with regard to i) geologic reasonableness, ii) ability to explain the variability in elevation of the unconformity, and iii) independence of residuals and predicted elevations.

i) Geologic reasonableness. The single plane model for the study area dips 0.06° N 81° W, discordant to structural trends for the region. The dual plane model defines planes which dip 0.09° S 39° E and 0.04° S 47° E (north and south of latitude 35° 45'N, respectively), and the direction of dip agrees closely with that of the underlying Tertiary and Cretaceous strata.

ii) Ability to explain elevation variability. Owing to the relief on this unconformity, a high percentage of the variability in elevation cannot be explained by any planar model. The single plane model explains 14 percent of the variability, and the dual plane model explains 43 percent and 32 percent to the north and south of latitude 35° 45'N, respectively. The superior ability of the dual plane model to explain elevation variability is evidence that the Plio-Pleistocene interval is

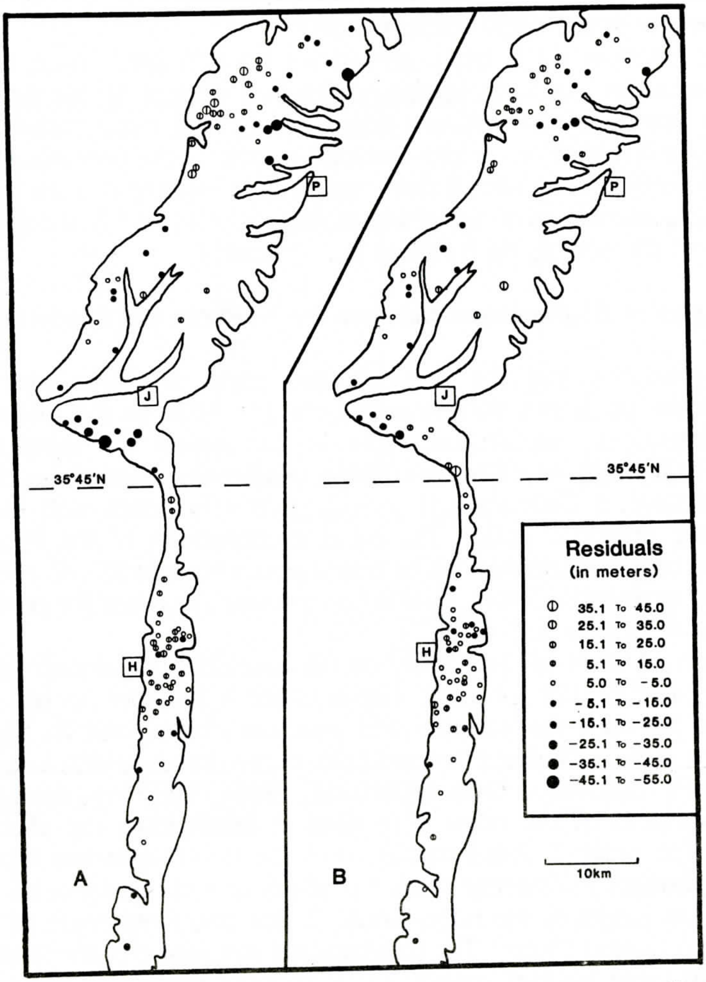

Figure 7. Locations of 104 lignite exploration drill holes on Crowley's Ridge from which elevations of the base of the Plio-Pleistocene interval were taken for multiple regression analysis. Each exploration hole location is assigned a symbol indicating the residual of the observed elevation with respect to the predicted elevation. A) Residuals for the single plane model. B) Residuals for the dual plane model (areas to the north and south of latitude 35° 45'N were analyzed separately). (H= Harrisburg; J= Jonesboro; P= Paragould).

faulted. For the dual plane model, the northern plane projects beneath the southern plane, suggesting down-to-the-north displacement.

iii) Independence of the residuals and predicted elevations. A strong pattern can be observed in the residual plot for the single plane model (Figure 8a). The dependence of the residuals and predicted elevations in this model suggests a poor fit to the actual geometry of the basal Plio-Pleistocene unconformity. Residual plots of the areas north and south of latitude 35° 45'N for the dual plane model show random scatter and constancy in the variance of the residuals (Figure 8b) reflecting a good fit to the geometry of the unconformity. This is further evidence that a dual plane (faulted) model is superior to a single plane (unfaulted) model.

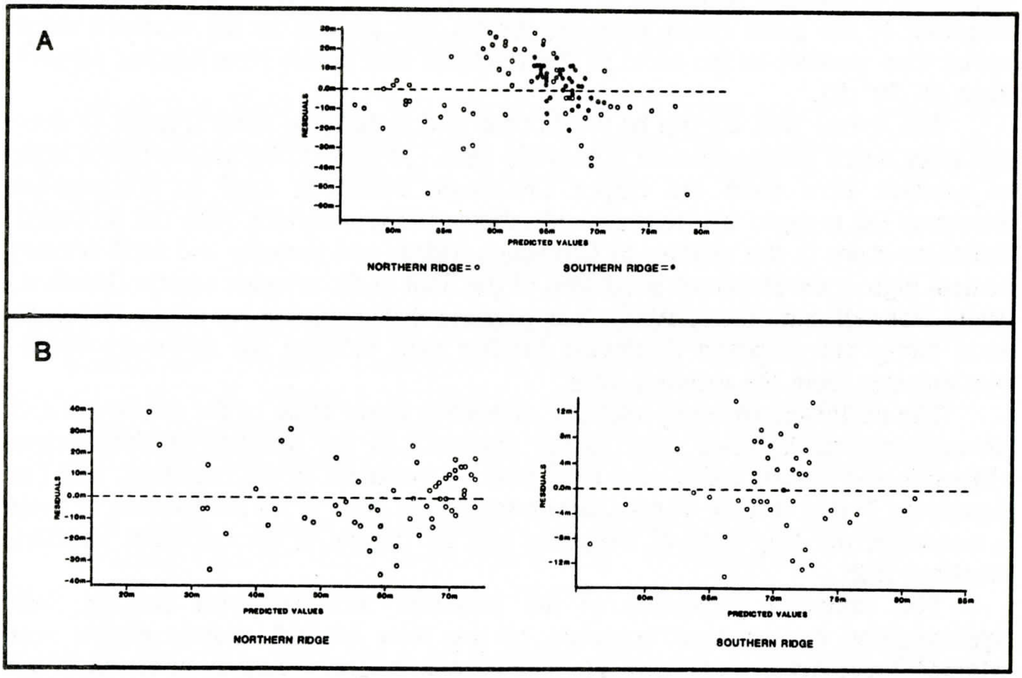

Figure 8. Residual plots for A) the single plane (unfaulted) multiple regression model, and B) the dual plane (faulted) multiple regression model.

DISCUSSION

A highly linear 19 km portion of the western margin of Crowley's Ridge trends N 61° W and extends from latitude 35° 45'N to latitude 35° 48'45"N (Figure 1). Fisk (1944) and O'Leary and Hildenbrand (1978) suggest that this linear margin of Crowley's Ridge is a fault. The abrupt change in geology of the ridge at latitude 35° 45'N suggests that gravel bearing Plio-Pleistocene deposits to the north have dropped adjacent to Eocene sands and clays to the south. If such is the case, then this linear feature is an inverted fault-line scarp supported by the more resistant Plio-Pleistocene gravel. The dual model planes described above for the northern and southern ridges are separated down-to-the-northeast by 52 m along this linear feature. Considering possible warping associated with faulting, this estimate of fault displacement is probably high.

Owing to low relief and poor exposure on Crowley's Ridge at latitude 35° 45'N, surface investigation of the Plio-Pleistocene and Eocene units cast no light on the question of the presence or absence of a fault. However, the direction of ground tilting suggested by the geomorphic analysis of the northern ridge (approximately S 65° E) is very nearly parallel to the strike of this proposed fault (N 61° W). If the fault is vertical, differential throw could result in east-southeast ground tilting.

Fissures associated with sand blows during the 1811-1812 New Madrid earthquakes were oriented N 30° E (Fuller, 1912), suggesting that this bearing is important in regional tectonics. The orientation N 30° E is parallel to the strike direction of the tilted block proposed herein and parallel to the northern ridge rather than parallel to the trend of the Reelfoot Rift or the New Madrid seismic zone (N 50° E).

The sparse well control of the Eocene and underlying units (Figure 4) does not offer much information on a possible fault. However, the southwestern limit of artesian flow from the Upper Cretaceous Nacatoch sand in northeastern Arkansas (as mapped by Boswell and others, 1965) coincides with the proposed fault-line scarp in the vicinity of Crowley's Ridge, and porosity and sand content remain high in the Nacatoch southwest of the limit of the artesian aquifer (Renfroe, 1949; Boswell and others, 1965). It is possible that displacement of the Nacatoch sand along the proposed northwest striking fault isolated the down-dip southwestern area from the recharge area.

The northwest trending interface of normal lower crust to the southwest and anomalously thick lower crust to the northeast in the Mississippi Embayment (Mooney and others, 1983) may be a zone of weakness in the basement, and the Jonesboro Pluton (Figure 4) may have intruded the crust at the intersection of such a northwest trending zone of weakness and the margin of the northeast trending Reelfoot Rift.

The southeast projection of the proposed west-northwest striking fault approximates the southern boundary of the New Madrid seismic region near Marked Tree, Arkansas (Figure 4). The seismic region is largely confined to the center of the Reelfoot Rift zone and geophysical data evidence Cenozoic uplift associated with the seismic region (Howe and Thompson, 1984). Structural contours on the base of the Eocene interval corroborate that the southeast regional dip has been disrupted by uplift in the vicinity of the seismicity. Figure 4 suggests that the uplift is restricted to the area northeast of the proposed fault. How this uplift is related to the down-to-the-northeast faulting suggested at Crowley's Ridge is problematic. At the risk of over speculation, perhaps slight isostatic adjustment occurred down-to-the-northeast in response to uplift and crustal shortening in the New Madrid seismic region.

The presence of a northwest trending structural discontinuity may also explain why the principal zone of seismicity stops near Marked Tree, Arkansas (Figure 4) and why some of the strongest seismicity occurs at that point (Johnston, 1982).

SUMMARY AND CONCLUSIONS

The geomorphic and geologic changes that occur abruptly at latitude 35° 45'N on Crowley's Ridge are interpreted as evidence that the areas to the north and south of this point overlie separate crustal blocks with differing Late Tertiary and Quaternary tectonic histories. A 19 km segment of the western margin of the ridge striking N 61° W is interpreted as an inverted fault-line scarp dividing these two areas. Projection of this proposed structural discontinuity appears to define the southern limit of the New Madrid seismic zone.

This investigation shows that an interpretation of Quaternary ground tilting can be important information in understanding the tectonic history and seismic potential of the Mississippi Embayment. Similar geomorphic studies elsewhere may be useful in defining tectonic elements in the New Madrid region.

ACKNOWLEDGEMENTS

I thank R.B. VanArsdale, M.J. Guccione, S.A. Schumm and R.G. Stearns for their assistance, discussion and review of the manuscript. Thanks to C.E. and S.W. Carlton, R.A.B. Leschen, R.C. Berg, K. Era, T. Arnold and S. Allen for assistance and advice.

REFERENCES

Adams, J., 1980, Active tilting of the United States midcontinent: geodetic and geomorphic evidence: Geology, v. 8, p. 442-446.

Boswell, E.H., G.K. Moore, L.M. MacCary and others, 1965, Cretaceous aquifers in the Mississippi embayment: U.S. Geol. Sur. Prof. Paper 448-C, 37p.

Call, R.E., 1889, The geology of Crowley's Ridge: Annual report of the Geol. Sur. of Ark., 283 p.

Fisk, H.N., 1944, Geologic investigation of the alluvial valley of the lower Mississippi River: U.S. Army Corps of Eng., Vicksburg, Miss., 78p.

Fuller, M.L., 1912, The New Madrid earthquake: U.S. Geol. Sur. Bull. 494, 119 p.

Guccione, M.J., W.L. Prior and E.M. Rutledge, 1986, The Tertiary and Quaternary geology of Crowley's Ridge; a guidebook: Ark. Geol. Comm., 39 p.

Halley, B.R., 1976, Geologic map of Arkansas: Ark. Geol. Comm., 1:500,000 scale.

Hildenbrand, T.G., M.F. Kane and J.D. Hendricks, 1982, Magnetic basement in the upper Mississippi Embayment region - a preliminary report, *In* Investigations of the New Madrid, Missouri earthquake region (F.A. McKeown and C.C Pakiser, eds.): U.S. Geol. Sur. Prof. Paper 1236, p. 39-54.

Holbrook, D.F., 1980, Arkansas lignite investigations - a preliminary report: Ark. Geol. Comm., 157 p.

Horton, R.E., 1945, Erosional development of streams and their drainage basins; hydrophysical approach to quantitative morphology: Geol. Soc. of Am. Bull., v. 56, p. 275-370.

Howe, J.R. and T.L. Thompson, 1984, Tectonics, sedimentation, and hydrocarbon potential of the Reelfoot Rift: Oil and Gas Jour., v. 82, no. 12, p. 179-190.

Johnston, A.C., 1982, A major earthquake zone on the Mississippi: Sci. Am. v. 246, p. 60-68.

Meissner, C.R., 1984, Stratigraphic framework and distribution of lignite on Crowley's Ridge, Arkansas: Ark. Geol. Comm. Info. Cir. 28-B, 14 p.

Mooney, W.D., M.C. Andrews, A. Ginzburg, D.A. Peters, and R.M. Hamilton, 1983, Crustal structure of the northern Mississippi Embayment and a comparison with other continental rift zones: Tectonophysics, v. 94,

p. 327-348.
Murray, G.E., 1961, Geology of the Atlantic and Gulf coastal province of North America: Harper and Brothers, New York, 692 p.
O'Leary, D.W. and T.G. Hildenbrand, 1978, Structural significance of lineament and aeromagnetic patterns in the Mississippi embayment: Proc. of the 3rd Internat. Conf. on Basement Tectonics, 1978, Durango, Colorado, p. 305-313.
Parker, R.S., 1977, Experimental study of drainage basin evolution and its hydrologic implications: Colorado State Univ., Fort Collins, Colo., Hydrology Paper 90, 58 p.
Potter, P.E., 1955, The petrology and origin of the Layfayette gravel: Jour. of Geol., v. 63, p. 1-38 and p. 115-132.
Price, R.C. and K.N. Whetstone, 1977, Lateral stream migration as evidence for regional geologic structures in the eastern Gulf coastal plain: Southeastern Geology, v. 18, p. 129-148.
Renfroe, C.A., 1949, Petroleum exploration in eastern Arkansas with selected well logs: Ark. Resource and Development Commission, Div. of Geol., Bull. 14, 159 p.
Saucier, R.T., 1974, Quaternary geology of the lower Mississippi Valley: Ark. Arch. Sur. Research Series no. 6, 26 p.
Schumm, S.A., 1986, Alluvial river response to active tectonics In : Active tectonics: National Academy Press, Washington, D.C., p. 80-94.
Stauder, W., R. Herrmann, S. Singh, R. Perry, E. Haug and S.T. Morrissey, 1979, Central Mississippi Valley earthquake bulletin: St. Louis Univ. Quarterly Report no. 21, 28 p.
Stephenson, L.W. and A.F. Crider, 1916, Geology and ground waters of northeast Arkansas: U.S. Geol. Sur. Water-Supply Paper 399, 315 p.
Strahler, A.N., 1952, Dynamic basis of geomorphology: Geol. Soc. of Am. Bull., v. 63, p. 923-938.
Zoback, M.D., R.M. Hamilton, A.J. Crone, D.P. Russ, F.A. McKeown, and S.R. Brockman, 1980, Recurrent intraplate tectonism in the New Madrid seismic zone: Science, v. 209, p. 971-976.

CORONA STRUCTURES: KEY TO THE RECOGNITION OF GRENVILLE BASEMENT WITHIN THE PINE MOUNTAIN WINDOW, GEORGIA

ALICE L. STIEVE — *Dept. of Geological Sciences, University of South Carolina, Columbia, SC 29208*

WILLIAM B. SIZE — *Geology Dept., Emory University, Atlanta, GA 30322*

ABSTRACT

The rocks within the Pine Mountain Window in the southern Appalachian Piedmont are interpreted as Grenville-age, granulite facies basement unconformably overlain by a lower Paleozoic amphibolite facies metasedimentary cover sequence. Distinguishing basement from cover is difficult because Paleozoic amphibolite facies metamorphism has overprinted and obscured the granulite facies mineral assemblages. In some places corona structures rimming relict hypersthene represent, mineralogically, the amphibolite facies overprint event in the basement. In other places, nests of amphibolite facies minerals, reminiscent of these coronas, are taken as an indication that the rock is in fact basement and that the granulite facies minerals have been completely retrograded. The presence of coronas or the relict coronas are a useful criteria for discerning basement rock from its metasedimentary cover.

INTRODUCTION

Identification of Precambrian basement rock becomes difficult when the original nature of the contact between basement rocks and cover is obscured by highPgrade metamorphism, folding and faulting. Radiometric dates are frequently unavailable and when available do not always yield unequivocal results. Inability to distinguish orthogneisses from paragneisses in high-grade orogenic terranes further complicates the understanding and the significance of Pb/U zircon dates. Therefore other criteria need to be developed for the recognition of basement. In this paper we characterize several types of corona structures in basement rock types and examine their distribution in portions of the Pine Mountain Window. After making the connection between the corona structures and Grenville granulite facies basement we then apply this criteria to the mapped section (southern half of the Johnstonville Quadrangle) in order to determine the distribution of basement rock (Figure 1,2,3).

REGIONAL GEOLOGY

The Pine Mountain Window, on the eastern edge of the Southern Appalachian Piedmont has been interpreted by previous investigators as granulite

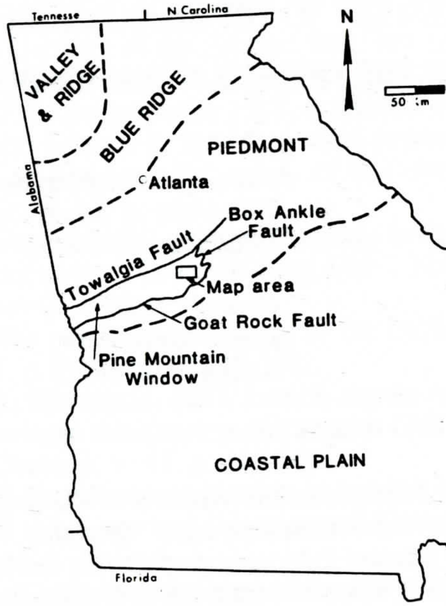

Figure 1. Outline map of Georgia showing the fault boundaries of the Pine Mountain Window and the map area.

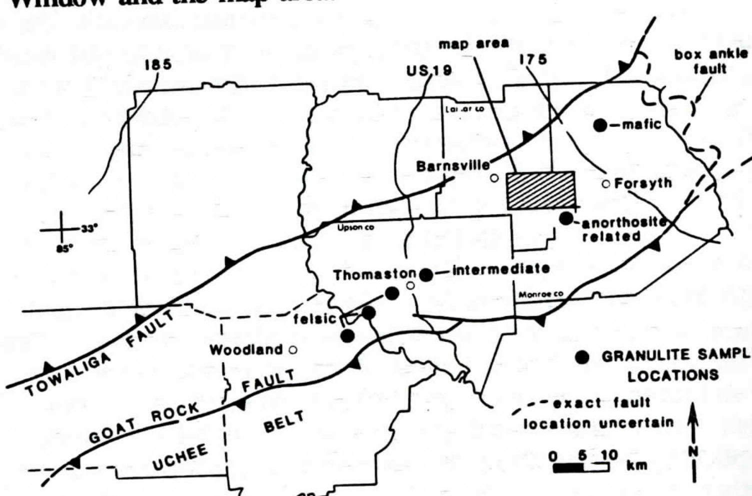

Figure 2. Locations of additional granulite facies rocks discussed in text (indicated by •). Map area indicated by hachured rectangle.

facies, probable Grenville-age, North American basement unconformably overlain by an amphibolite facies lower Paleozoic cover sequence (Clarke, 1952; Sears and Cook, 1984; Kish and others, 1982; Odom and Kish, 1973). The basement and cover sequence were folded into a series of stacked, overturned nappes with the basement residing in the cores of these nappes (Sears and Cook, 1984; Sears and others, 1983; Schamel and Bauer, 1980) (Figure 4). The Pine Mountain Window is separated from other Piedmont rocks by several major faults of differing ages (Hooper, 1986; Sears and others, 1983; Sears and Cook, 1984; Schamel and Bauer,

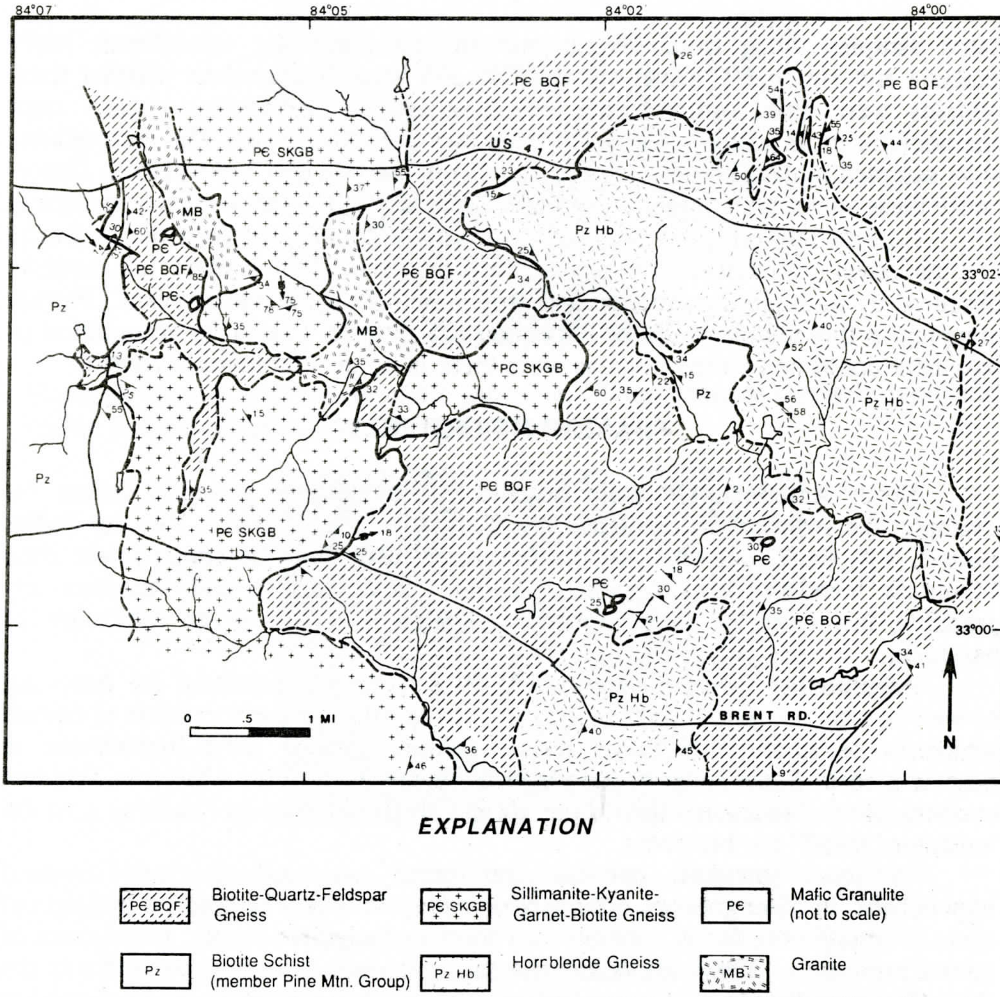

Figure 3. Reconnaissance map of southern half of Johnstonville Quadrangle.

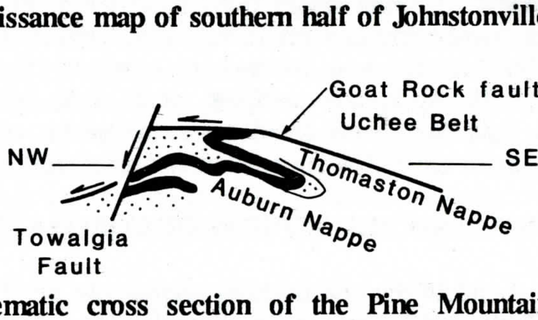

Figure 4. A schematic cross section of the Pine Mountain Window in the Thomaston, Ga. vicinity from Sears and others, 1983. Black: Hollis quartzite; Stippled: Pine Mountain Group; Clear: basement.

1980) (Figure and 2). The gneisses and schists within the window reflect medium (amphibolite facies) to high-grade (granulite facies) metamorphism. Kish and others (1982) dated the Woodland Gneiss in the Pine Mountain Window at 1,055 ±10 Ma. This gneiss was interpreted as an orthogneiss. Odom and Kish (1973) dated samples taken from several gneissic lithologies by wholeProck Rb/Sr analysis and zircon U/Pb analysis at 1,080 ±20 Ma. It is unclear whether these samples were from orthogneisses or paragneisses. Additional zircons from charnockitic rocks were dated by U/Pb method at 1100 ±20 Ma. The charnockites were sampled in the Thomaston area, in the area mapped by Clarke (1952). Importantly these rocks are Grenville-age basement rocks that contain corona structures.

Current interpretation holds that the initial contact between the basement and its cover rocks was unconformable. However, this contact has become obscured by multiple defomation and amphibolite facies metamorphism. Further mapping in this region would be expedited if a reliable criteria for recognition of basement could be applied in areas were there is no geochronologic control.

BASEMENT CRITERIA

North American Grenville basement is commonly granulite facies, for example; the Adirondack highlands, the Baltimore Gneiss Dome, PA, the Pedlar Massif, VA, the Canadian Grenville Province. The dated basement in the Pine Mountain Window contains relict granulite facies phases and therefore any granulite facies in the Pine Mountain Window is taken as an indication of basement.

Amphibolite facies metamorphism subsequently overprinted the basement as well as prograding the cover sequence. This resulted in the formation of corona structures of amphibolite facies phases forming around relict hypersthene in basement rock. Since some of the dated basement in the Pine Mountain Window contains corona structures then these corona structures may be taken as a useful indicator "fossil" for basement.

In some gneisses, coronas are intact and well developed around hypersthene, in other gneisses orthopyroxene may no longer be present, but clots or nests of amphibolite facies minerals may form as distinctive shapes, reminiscent of corona structures. These knots are also taken as an indicator of basement in the Pine Mountain Window. Corona and/or relict corona structures are here used to determine basement distribution in a small, recently mapped area(southern half of the Johnstonville Quadrangle) near the eastern terminus of the Pine Mountain Window (Figure 1,2,3). Additional samples were taken from other basement outcrop areas that have not been dated by radioisotope analyses. Thus the description of coronas in the following section is drawn from a larger region.

DISTRIBUTION AND DESCRIPTION OF CORONA STRUCTURES

Coronas are found in the charnockitic gneisses in the Thomaston, Georgia area, mapped by Clark (1952) (Figure 2). Samples for Odom and Kish's (1973) date come from these gneisses. Coronas are also observed in intermediate composition gneisses (enderbitic to mangeritic) immediately to the east of the Thomaston area; in mafic rocks northeast of Forsyth, Georgia and in mafic rocks associated with anorthosite immediately south of the map area. Within the map area, coronas are found in mafic rocks that occur as small conformable pods within a biotite-quartz-feldspar gneiss (Figure 3). In this paper mineral modifiers are listed in order of increasing abundance.

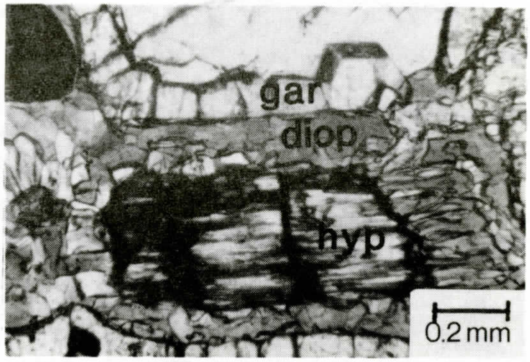

Figure 5. Corona structure in mafic granulite. Clinopryroxene replaces hypersthene (plane polarized light). See chemical reaction in text.

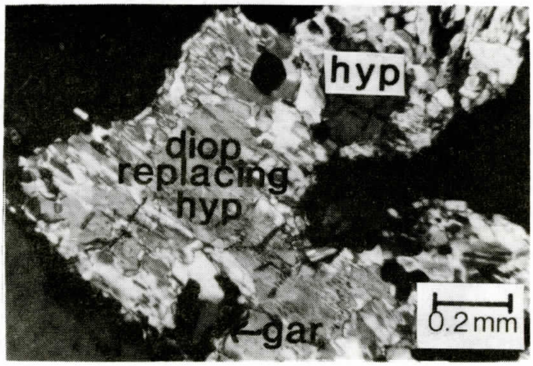

Figure 6. Hypersthene being replaced by clinopyroxene in a mafic granulite (x-nicols).

The variety of coronas range from perfect concentric rings of minerals to symplectic knots of "outer ring" minerals which have entirely replaced any core or "inner ring" minerals. Core minerals include; hypersthene, clinopyroxene, ilmenite/magnetite, olivine. Hypersthene is typically rimmed and replaced by clinopyroxene (Figure 5 and 6). Biotite or garnet replacement of hypersthene is less common. Olivine is rimmed with amphibole. Clinopyroxene and ilmenite/magnetite are rimmed by garnet (Figure 7). The opaque grains are less commonly rimmed with biotite or a garnet/biotite symplectite.

In the mafic granulites, corona associations include (core mineral on the left):

Opaque-garnet-biotite-plagioclase
Opaque-sphene-clinopyroxene-plagioclase
Orthopyroxene-clinopyroxene-garnet-plagioclase
Olivine-amphibole-garnet-plagioclase
Plagioclase-garnet
Clinopyroxene-amphibole-garnet

Charnockites from the Thomaston area contain hypersthene grains, which are embayed and partially replaced by clinopyroxene. Most grains of hypersthene

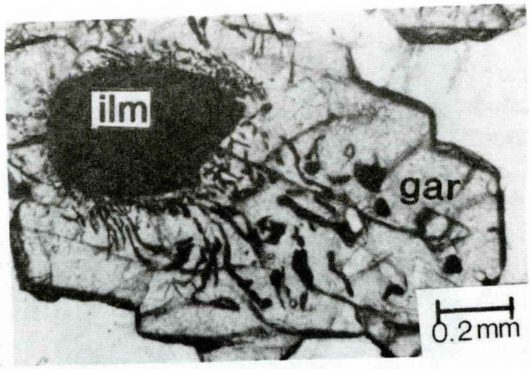

Figure 7. Ilmenite "replaced" by garnet. Worms of ilmenite dispersed through garnet corona (plane polarized light).

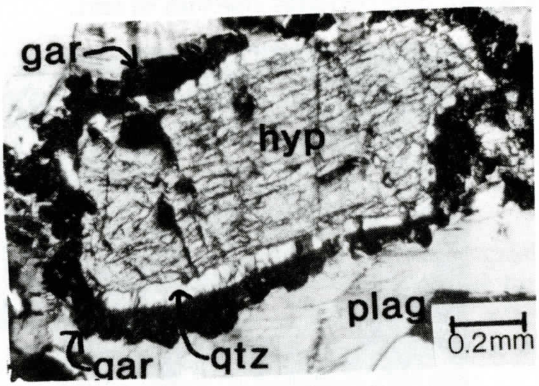

Figure 8. Corona structure in felsic granulite (charnockite) from the Thomaston area, x-nicols. Clinopyroxene is missing from these coronas.

are surrounded by a double corona of quartz and garnet (Figure 8) or reside in large clots of other mafic minerals; garnet biotite, clinopyroxene and ilmenite. Corona associations in the felsic granulites, include (core mineral on the left):

Orthopyroxene-quartz-garnet-plagioclase

Orthopyroxene-clinopyroxene-garnet-plagioclase

The geometric arrangement of these coronas implies formation in the solid state under static tectonic conditions. The coronas represent a chemical reaction between minerals which did not proceed to equilibrium. It is possible, therefore, to identify probable reactants and products. One particularly common corona structure, the orthopyroxene-clinopyroxene-garnet-plagioclase association, appears to follow a reaction similar to one reported by Green and Ringwood (1967):

$$\underset{\text{orthopyroxene}}{4(Mg,Fe)\,SiO_3} + \underset{\text{anorthosite}}{CaAl_2Si_2O_8} = \underset{\text{garnet}}{(Mg,Fe)_3Al_2Si_3O_{12}} + \underset{\text{clinopyroxene}}{Ca(Mg,Fe)Si_2O_2} + SiO_2$$

In the study area, garnet is in textural equilibrium with the clinopyroxene. The garnet grains occur as embayments into plagioclase grains and the plagioclase has distinct concentric zonation. Clinopyroxene replaces orthopyroxene. The clinopyroxene is in a granular symplectite with quartz. This reaction and others observed in the Pine Mountain Window represent a granulite facies event with an amphibolite facies overprint. For example the formation of sphene in the opaque-sphene-clinopyroxene-plagioclase association is consistent with an amphibolite facies overprint.

Wagner and Crawford (1975) found that the garnet present in coronas forming around various minerals in any one rock are uniform in composition throughout that rock. Thus there must be solution transfer of ions to accommodate the large differences in the Mg and Fe content orthopyroxene or clinopyroxene or magnetite among the hypersthene-quartz-garnet coronas, hypersthene-diopside-garnet coronas and magnetite-garnet coronas in the same rock. Wagner and Crawford (1975) also contend that the optical zoning of plagioclase grains in association with garnet coronas is the result of Ca^{++} being taken up in the recrystallization of diopside. This was verified, in that study, with microprobe analysis of Ca^{++} content across the plagioclase grain boundary. Whitney (1978) also documented this effect. The Ca^{++} depletion in plagioclase near corona structures is a likely explanation for the observation of plagioclase zoning in the high grade metamorphic rocks in the Pine Mountain Window. Alternatively, the high Ca^{++} cores, low Ca^{++} rims may be due to a reequilibration of the rim to an amphibolite facies overprint.

As previously stated, the corona structures represent a reaction which did not reach equilibrium. The intermediate composition granulites, sampled to the west of the map area (Figure 2), have poorly developed corona structure in that the corona minerals are not clearly arranged in concentric rings. However, symplectic intergrowths of garnet, clinopyroxene and biotite are seen in knots or domains within the rock. The geometry of these domains are reminiscent of the geometry of the corona structures. These symplectites may represent an end member texture which evolved from a corona. In other words, they may represent the completion of the amphibolite facies reaction.

BASEMENT IN THE MAP AREA

The distribution of corona structures in the mapped section is limited to the conformable mafic pods and other mafic rocks associated with an anorthosite body, all within the biotite-quartz-feldspar gneiss and possibly the sillimanite-kyanite-garnet-biotite gneiss. Modes for the different lithologies are given in Table 1.

Biotite-Quartz-Feldspar Gneiss

Peak metamorphic conditions for the biotite-quartz-feldspar (BGF) gneiss reached sillimanite zone of the upper amphibolite facies, possibly granulite facies. Evidence to support this include; rare hypersthene, myrmekite, metamorphic K-feldspar with perthitic texture (Howie,1964) and stubby prisms of subhedral to euhedral sillimanite are present locally. The presence of sillimanite is consistent under granulite facies temperature and pressures with bulk chemistry high in Al_2O_3 (Thurston and Breaks, 1978; Turner, 1980).

The mafic rocks within the BQF gneiss contain granulite facies mineral assemblages with well developed coronas (Figure 9). These corona structures along with the high metamorphic grade of the enclosing BGF gneiss supports the interpretation that the GQF gneiss is basement.

Table 1. Modal Analyses 1000+ points/mode

Rock Type	*1*	*2*	*3*	*4*	*5*	*6*	*7*	*8*	*9*
N	7	5	3	2	2	2	6	1	2
Plagioclase	20.8	40.8	36.6	29.6	21.5	33.8	19.8	10.2	25.4
(An)	32	41	75	38	59	37	30.		
K-Feldspar	40.2	20.7	4.0			26.3	34.1	21.5	38.4
Quartz	28.3	15.9	3.7	18.8	0.6	25.8	25.0	10.1	27.5
Garnet	3.6	8.6	11.4	20.0	21.0	3.7	9.2	14.3	
Orthopyroxene	1.4	3.0	15.5	6.6		tr.			
Clinopyroxene	1.3	1.7	25.4	12.5	11.8		0.1		
Hornblende	tr.	0.8	tr.	tr.	35.2		2.4	tr.	
Biotite	3.2	6.7	0.3	6.4	1.2	10.8	6.4	22.7	7.0
Opaque	1.1	1.8	3.7	5.3	5.6	0.5	0.6	1.2	
Apatite	tr.	0.1	0.1	0.1	tr.	tr.	0.1	0.2	0.1
Muscovite									1.0
Kyanite[1]								10.1	
Misc.	0.6	2.8	0.9	0.2	2.3[2]	1.1	1.8	9.8[3]	0.5
Perthite	+	+	-	-	-	+	+	-	-
Corona[4]	++	+	++	++	++	-	-	+	-
Myrmekite	+		+	-	-	-	+	-	-

+/- presence or absence
1 - charnockites from Thomaston Quadrangle
2 - intermediate composition granulites from Logtown Quadrangle
3 - mafic granulite (NE Forsyth Quadrangle)
4 - mafic granulite associated with anorthosite, study area
5 - mafic granulite, Johnstonville Quadrangle
6 - biotite-quartz-feldspar gneiss, study area
7 - hornblende gneiss, study area
8 - sillimanite-kyanite-garnet-biotite gneiss, study area
9 - muscovite-biotite granite, study area
superscripts
1 - kyanite + trace sillimanite
2 - olivine
3 - alteration material
4 - ++ coronas, + symplectic knots

Sillimanite-Kyanite-Garent-Biotite Gneiss

The sillimanite-kyanite-garnet-biotite gneiss (SKGB gneiss) attained at least upper amphibolite facies but it is so highly sheared and strained the textural evidence of corona structures or corona relicts has been obscured, if it ever existed. The gneiss contains euhedral to subhedral, felted kyanite. Trace sillimanite is adjacent to kyanite and appears to be replaced by the kyanite. The shear fabric is

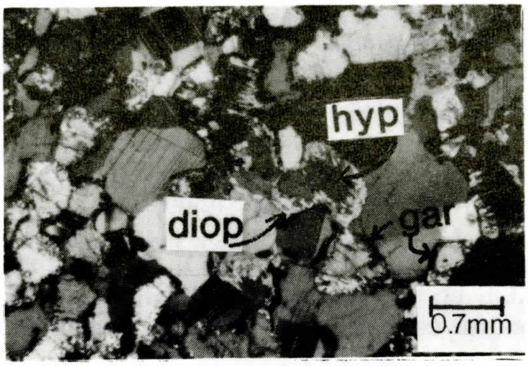

Figure 9. Granoblastic texture in mafic granulite, Corona association involves hypersthene, clinopyroxene and garnet (x-nicols).

characterized by; chaotic foliation; strained and fractured quartz grains that have been elongated into thin ribbons (uniform orientation at microscopic scale); heavily fractured porphyroblastic garnet typically penetrated by recrystallized biotite. The lens shaped symplectites of garnet, biotite and kyanite (Figure 10) may be relict coronas that have been extensively distorted and further recrystallized. Thus the SKGB gneiss may be a part of the basement complex.

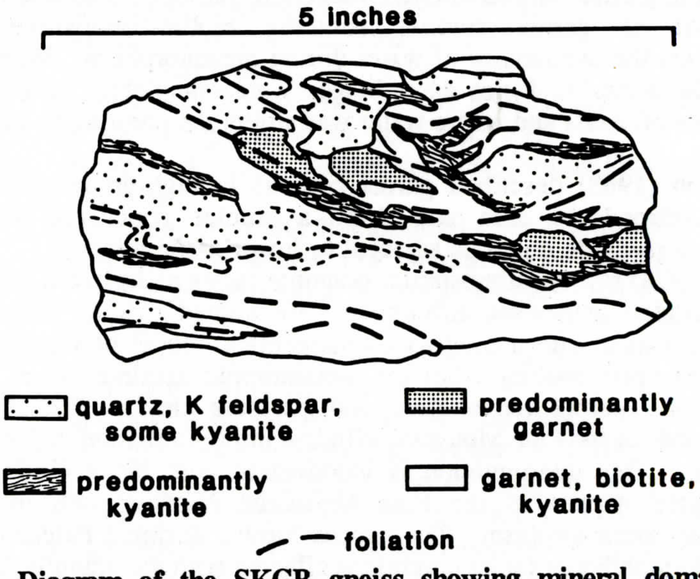

Figure 10. Diagram of the SKGB gneiss showing mineral domains or flaser structure and foliation form lines.

Hornblende Gneiss

The hornblende gneiss (Hb gneiss) reached amphibolite facies; apatite grains surrounded by sphene, knots of porphyroblastic garnets, perthitic K-feldspar, zoned plagioclase support this conclusion. The Hb gneiss was also tectonically strained, as porphyroclasts of feldspar are strained and mantled with tiny recrystallized (annealed) feldspar grains. The gneiss is metamorphosed but there is no compeling evidence to place it with the basement. The garnet knots do not contain any clinopyroxene and do not resemble the relict coronas of the basement even geometrically.

Muscovite-Biotite Granite

The muscovite-biotite granite (MB granite) is the youngest rock in the map area. It intrudes the SKGB gneiss (xenoliths of the SKGB gneiss are observed in the MB granite) and contains essentially no foliation. It clearly is not a part of the basement.

DISCUSSION

There are other Precambrian basement terranes along the east coast of the North America which have been reported to contain coronas in granulite facies rocks.

Wagner and Crawford (1975) reported garnet coronas in granulite facies rocks of the Baltimore Gneiss in south east Pennsylvania. They concluded that the coronas developed during a retrograde amphibolite facies event. A gradual sequence from thin garnet coronas through thickening garnet coronas and finally to the development of garnet coronas rimming biotite-clinopyroxene-quartz sympletites reflects the availability of water during metamorphism. Where water was available the granulite facies assemblages were completely retrograded to amphibolite facies minerals and where water was absent the coronas developed and remained.

Buddington (1963) described garnet coronas in high-grade meta-igneous rocks in the Adirondacks area and drew a similar conclusion about the juxtaposition of high-grade minerals adjacent to lower-grade minerals.

Whitney(1978) investigating similar granulite facies rocks in the Adirondack Highlands, concluded somewhat differently. He argued that an intact corona structure is inconsistent with a prograde, synkinematic model of metamorphism. The garnet forms upon cooling, after the metamorphic maxima, when the rock passes through the garnet temperature and pressure field. The intact and undeformed coronas of the Pine Mountain Window imply formation in deep-seated, static conditions. This interpretation is inconsistent with the evolution of the folded and faulted nappes of the Pine Mountain Window with respect the amphibolite facies metamorphism. The nappes formed during a Paleozoic island arc collision and amphibolite facies conditions effected both the granulite basement and its cover rocks at that time (Schamel and Bauer, 1980). The basement cores of these nappes had apparently not taken up the bulk of the strain during nappe emplacement.

CONCLUSIONS

Previous investigators have interpreted the structure of the Pine Mountain Window to be an overturned, attenuated and faulted nappe sequence. Granulite facies Precambrian basement cores these nappes with the cover sequence residing on the limbs or in the synforms. The nappes formed during a Paleozoic island arc collision and amphibolite facies conditions effected both the granulite facies basement and its cover rocks. The amphibolite facies event is a retrograde phenomenon in the basement resulting in the formation of corona structures of amphibolite facies minerals rimming the granulite facies core minerals. The cover sequence was prograded to amphibolite facies and would not reflect granulite facies or be expected to develop corona structures. The criteria of the presence of coronas in identifying basement rock in the Pine Mountain Window may be valid in other complex basement terranes when used in conjunction with other independent petrographic criteria or with the structural relationships of the region.

REFERENCES

Buddington, A.F., 1963. Isograds and the role of H_2O in metamorphic facies of orthogneisses of the NW Adirondack area, N.Y.: Geol. Soc. Am., Bull., v. 74, p. 1155-1181.

Clarke, J.W., 1952, Geology and mineral resources of the Thomaston Quadrangle, Ga.: Ga. Geol. Survey Bull. #59, 99pp.

Green, D.H. and Ringwood, A.E., 1967, The genesis of basaltic magmas: Min. and Pet., v.15, p. 103.

Hooper, R.J., 1986, Geologic studies at the east end of the Pine Mountain Window and adjacent piedmont, central Georgia: PhD dissertation, Univ. of South Carolina, Columbia, SC., 29208, 322 pp.

Howie, R.A., 1964, Charnockites: Sci. Progr., London, v. 52, p. 628-644.

Kish, S.A., Fullagar, P.D., Odom, A.L., 1982, 95th Annual Meeting, Geol. Soc. Am., Abs. with Programs, v. 14, no. 7, p. 530.

Odom, A.L. and Kish, S., 1973, Technical Files, Georgia Geologic Survey, Atlanta, Georgia.

Schamel, S. and Bauer, D., 1980, Remobilized Grenville basement in the Pine Mountain Window, *in* Wones, D.R. (editor), The Correlation Program Project 27: Caledonide orogen. Virginia Sciences Memoir #2, p. 313-316.

Sears, J.W. and Cook, R.B., Jr., 1984, An overview of the Grenville basement complex of the Pine Mountain window, Alabama and Georgia: Geol. Soc. Am. Special paper 194, p.281-287.

Sears, J.W. and Cook, R.B., Gilbert, O.E., Jr., Carrington, T.J., Schamel, S., 1983, Stratigraphy and structure of the Pine Mountain Window in Georgia and Alabama, *in* Wigley, P.B. (editor), Latest thinking on the stratigraphy of selected areas in Georgia: Georgia Geol. Survey, Infor. Cir. 54-A, p.41-53.

Thurston, P.C. and Breaks, F.W., 1978, Metamorphic and tectonic evolution of the Uchi-English River Subprovince, in Metamorphism in the Canadian Shield: Geol. Sur. Canada, Paper 78-10, p. 49- 62.

Turner, F.J., 1980, Metamorphic Petrology, Mineralogical , Field and Tectonic Aspects: 2nd ed., Hemisphere Publ. Co., N.Y., 694 pp.

Wagner, M.E., and Crawford, M.L., 1975, Polymetamorphism of the Precambrian Baltimore Gneiss in southeastern Pennsylvania: Am. Jour. Sci.,v. 275, P. 653-682.

Whitney,P.R., 1978, The significance of garnet isograds in granulite facies rocks of the Adirondacks, in Metamorphism in the Canadian Shield: Geol. Survey

Canada, paper 78-10, p. 357-366.

BIONT TRANSITION SEQUENCES IN THE JOHNSON POINT *CREPIDULA* BIOSTROME, EARLY PLEISTOCENE OF NORTH CAROLINA

WILLIAM MILLER, III

Geology Department and Marine Laboratory
Humboldt State University, Arcata, CA 95521

ABSTRACT

Shells forming a *Crepidula fornicata* biostrome within the early Pleistocene James City Formation were encrusted and bored by a variety of "fouling" organisms. Early stages of biont transition sequences on *Crepidula* shells began with *Spathipora* and *Terebripora*, which are the borings of branching rhizome-like ctenostome bryozoans. Middle stages in transition sequences consisted of many different organisms with varied modes of life. These included borers (the endolithic polychaete worm, *Polydora*; a possible alga, ?*Gomontia*; a demosponge, ?*Cliona*), sheet-like colonies of cheilostome bryozoans (mostly *Cyclocolposa* and *Cribrilina*), and a problematic epilithic organism (possibly an alga or bryozoan, preserved as brown branching lines on shells). Late stages were dominated by epilithic cheilostome zoaria that gradually overgrew organisms that were important in the earlier stages. Dominance by late-stage cheilostomes was occasionally disrupted by local disturbances that re-opened shell substrata to colonization by comparatively less successful space-competitors.

INTRODUCTION

A cursory examination of larger mollusks from a snail bank dominated by *Crepidula fornicata* (Linné) within the James City Formation reveals an apparently regular succession of bionts (epi- and endolithic organisms infesting shells). The succession pattern seems to always begin with ctenostome bryozoans, which are followed by polychaete worms, and ends with cheilostome bryozoans. In terms of biont morphology, the sequence appears to begin with pioneering colonial organisms that spread over shells by means of branching "runners", followed by tubular borings of solitary non-colonial organisms, which are in turn overgrown by colonial organisms organized in extensive sheets that eventually dominated shell surfaces if growth was uninterrupted by natural disturbances. However, if a random sample of shell substrata is examined carefully, a more complex and less regular sequence of biont transitions is noted. This more detailed picture involves both a richer association of epi- and endolithic species, as well as a more intricate and stochastic pattern of transitions. In this paper I will describe the transition sequence of so-called "fouling" organisms that inhabited *C. fornicata* shells forming an early Pleistocene biostrome at Johnson Point, Craven County, eastern North Carolina (Figure 1). I also illustrate a simple method of characterizing such transitions.

Short-lived biont transitions of the type described here may encompass time spans of only years to tens-of-years, at most. They are among the briefest synecologic processes resolvable in fossil samples. Microsuccession on shell surfaces can be driven by biotic interactions (e.g., competition, predation). For

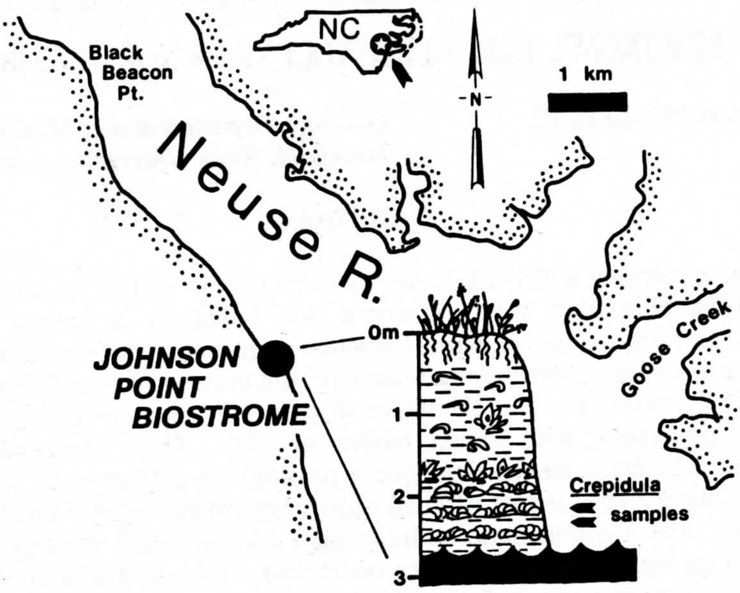

Figure 1. Location map and stratigraphic section.

this reason, biont transition patterns preserved on large fossil shells could be the only available source of information on original ecologic associations in fossil deposits in which time-averaging and bioturbation are important factors in surrounding sediments. In such cases, interspecific interactions may be preserved only on shells that hosted fouling communities. Factors influencing short-term transition sequences on these shell islands include: 1) availability of suitable substrata on what may be an otherwise uninhabitable seafloor; 2) supply of epi- and endobiont propagules and substratum selection behavior; 3) intra- and interspecific competition (usually for space); 4) predation; 5) mutualistic interactions; 6) astogeny and ontogeny of species involved in transitions; and 7) abiotic factors such as temperature, oxygen tension, salinity, turbidity and hydraulic energy (see Jackson, 1983). It is also clear that disturbance regime plays a role in development of transition sequences (Sousa, 1985; Connell and Keough, 1985). More or less regular or recurrent colonization sequences, beginning and ending repeatedly with the same kinds of organisms, probably represent small-scale community temporal dynamics propelled largely by biotic interactions (e.g., Wilson, 1985; Bailey and Tedesco, 1986).

METHODS

Many papers describe fouling communities on modern and fossil shells, yet few studies outline the methods of determining transition sequence where more than one outcome is possible for each step in a sequence. In cases where succession is a probabilistic process, because of variation in factors such as recruitment dynamics, results of competitive interactions, or small-scale natural disturbances, there is a need to characterize the "average transition sequence". This problem can be approached by applying the method of sequence analysis used in studies of sedimentary facies transitions (Selley, 1969; Reading, 1978). The technique allows visualization of the frequency of individual transitions by comparing the observed transitions with those expected when a random pattern is assumed (Figure 2).

Bionts	A	B	C	D	Row sums:
A	5	10	3	1	19
B	8	3	2	2	15
C	5	4	0	1	10
D	1	0	0	1	2
Column sums:	19	17	5	5	46

STEP 1.

OBSERVED BIONT TRANSITIONS; TAXA AT TOP OF COLUMNS CROSS-CUT OR OVERGREW THOSE LISTED AT END OF ROWS (E.G., BIONT 'B' OVERGREW 'A' IN 10 INSTANCES IN THE SAMPLE).

	A	B	C	D
A	8	7	2	2
B	6	6	2	2
C	4	4	1	1
D	1	1	0	0

STEP 2.

TRANSITION ARRAY WHEN RANDOM PATTERN IS ASSUMED. (VALUES CALCULATED BY MULTIPLYING COLUMN TOTALS BY ROW TOTALS AND THEN DIVIDING BY GRAND TOTAL, 46.)

	A	B	C	D
A	-3	+3	+1	-1
B	+2	-3	0	0
C	+1	0	-1	0
D	0	-1	0	1

STEP 3.

DIFFERENCES BETWEEN THE OBSERVED BIONT TRANSITIONS (STEP 1) AND PREDICTED VALUES WHEN RANDOM PATTERN IS ASSUMED (STEP 2).

Figure 2. Method of constructing biont transition array shown in Figure 3 (based on Selley, 1969, Fig. 1).

For this study I selected a total of 60 mature (female or sexually transitional) *Crepidula fornicata* shells at random from two, 1-litre bulk samples collected at Johnson Point (Figure 1). Outer surfaces were examined using a dissecting microscope to locate and identify all epi- and endobionts. At the same time overgrowths and cross-cutting relationships among these organisms were recorded. Results are shown in Table 1. These data then were used to construct the transition array shown in Figure 3.

Table 1. Epi- and endobionts from outer surfaces of *Crepidula fornicata* shells in the Johnson Point biostrome. Up to five transition steps (distinguished by cross-cutting relationships or overgrowths) were observed. Taxa at top of list occurred in initial steps; those near bottom of list cross-cut or overgrew earlier arrivals. Numbers are counts based on occurrences on 60 shells, with underscoring to help visualize typical position of organism in transition sequences.

Taxon	Type organism	Substrate niche + feeding group	Morphology	Transition steps				
				1	2	3	4	5
Spathipora	Br*	ENSF	runners	38	-	-	-	-
Terebripora	Br*	ENSF	runners	21	-	-	-	-
Polydora	An*	ENSF	tubes	3	19	20	2	-
Cyclocolposa	Br	EPSF	sheets	1	4	16	4	-
?Gomontia	Al*	ENPP	galleries	1	17	1	-	-
Balanus	Ci	EPSF	cone	-	1	-	-	-
?Cliona	Po*	ENSF	galleries	-	11	9	-	-
Indet. brown branching lines	Br?, Al?	EPSF?	runners	-	15	1	-	-
Cribrilina	Br	EPSF	sheets	-	3	6	10	1
Electra	Br	EPSF	runners & sheets	-	1	2	-	-
Hippoporina	Br	EPSF	sheets	-	-	2	-	-
?Planobulina	Fo	EPSF?	"sheet"	-	-	-	1	-

Explanation:

* -- represented by borings or surface pits only

Type organism --

Br, Bryozoa
An, Annelida
Ci, Cirripedia
Po, Porifera
Fo, Foraminiferida
Al, alga

Substrate niche & feeding group --

ENSF, endolithic suspension feeder
ENPP, endolithic primary producer
EPSF, epilithic suspension feeder

STRATIGRAPHIC CONTEXT AND PALEOENVIRONMENT

Samples used in this study were collected from a *Crepidula* biostrome enclosed in mudstone within the early Pleistocene James City Formation. The Johnson Point locally was first described by DuBar and others (1974, p. 111), and is the focus of numerous recent paleontologic studies (Miller, 1986, 1987, in press; Zullo and Miller, 1986; Woods, 1987; Miller and DuBar, 1988). James City

	Spathipora	*Terebripora*	*Polydora*	*Cyclocolposa*	*?Gomontia*	*Balanus*	*?Cliona*	Indent. brown branching lines	*Cribrilina*	*Electra*	*Hippoporina*	*?Planorbulina*
Spathipora	0	0	-2	-6	+8	+1	0	+5	-5	0	-1	0
Terebripora	0	0	+1	-3	+3	0	+1	+4	-2	0	0	0
Polydora	0	0	-7	+6	-3	0	-1	-2	+7	+1	+1	0
Cyclocolposa	0	0	0	-1	0	0	0	0	+2	0	0	0
?Gomontia	0	0	+3	0	-3	0	+2	-2	-1	+1	0	0
Balanus	0	0	0	0	0	0	0	+1	0	0	0	0
?Cliona	0	0	+1	+3	-1	0	-2	-1	+1	0	+1	+1
Indent. brown branching lines	0	0	+3	+1	-2	0	0	-2	-1	0	+1	0
Cribrilina	0	0	+4	0	-2	0	+1	-1	-1	0	0	0
Electra	0	0	+1	0	0	0	0	0	0	0	0	0
Hippoporina	0	0	0	0	0	0	0	0	0	0	0	0
?Planorbulina	0	0	0	0	0	0	0	0	0	0	0	0

Figure 3. Difference between observed biont transitions and predicted values when random pattern is assumed, using data from the Johnson Point *Crepidula* biostrome. Array confirms, for example, that *?Gomontia* frequently succeeded early colonizing *Spathipora*; it was in turn succeeded by *Polydora*, which was then typically overgrown by *Cyclocolposa*.

deposits usually are regarded as time-equivalent to the Waccamaw Formation in southeastern North Carolina-northeastern South Carolina. This traditional correlation has been questioned by Cronin and other (1984) who think that the James City may be slightly younger, or in the range of 1.3 to 0.7 Ma. The *Crepidula* biostrome originated as a subtidal snail bank in a muddy-bottom, subtropical marine bay (DuBar and Howard, 1969; Blackwelder, 1981). For extensive discussion of age, depositional environment and paleoecology of the Johnson Point beds, see DuBar and others (1974), Miller and DuBar (1988), and Miller (in press).

DEVELOPMENT OF FOULING COMMUNITIES

A total of twelve different organisms (species or ichnospecies), mostly bryozoans, infested the *Crepidula* shells (Table 1). Six of these are represented only by borings or surficial color stains. In all, four animal phyla are represented, together with two protist groups.

The first stage or step in transition sequences is dominated by the ctenostome bryozoan borings *Spathipora* (Figure 4A) and *Terebripora* (Figure 4B). These names are applied by some workers to both borings and to the tracemaking dead. The same is true in cases where shells were thoroughly riddled by borings that penetrated to the interior spaces. There were no signs that biont propagules differentiated between open patches on live vs. dead shells. Availability of an unoccupied, suitable hard surface, and possibly presence of conspecific bionts, were the crucial factors.

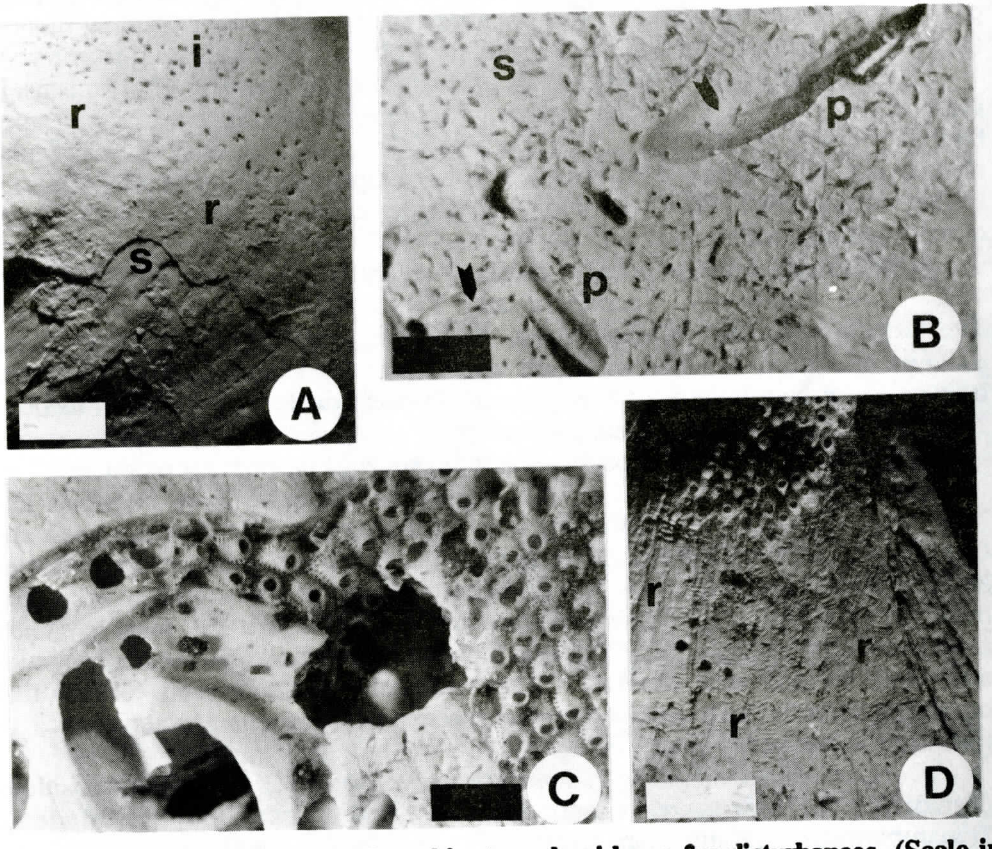

Figure 5. Reaction of *Crepidula* to bionts and evidence for disturbances. (Scale in A represents 3 mm; in B and D, 2 mm; in C, 1 mm.)
A. Rampart (r) secreted by living *Crepidula* to halt spread of endobiont infestation (i). Note uninfested shell surface (s) of subjacent member of the *Crepidula* stack.
B. *Spathipora* (s) overgrowing abandoned *Polydora* (p) borings (arrows).
C. *Cyclocolposa* overgrowing shell that was heavily infested with *Polydora*.
D. *Cyclocolposa* zoarium disturbed by grazing gastropod (?). Note radula scars (r) on shell surface below the colony.

It is not clear why ctenostomes always initiated colonization sequences. Although their early appearance may have resulted simply from availability of larvae, it is more likely *Spathipora* and *Terebripora* were attracted by feeding/respiration currents produced by living *Crepidula*. This is supported by occurrence of concentrations of ctenostome borings near the margins of host shells, and indirectly by presence of the $CaCO_3$ shields and ramparts that seem to have served to prevent spread of ctenostome zoaria (Figure 5A). Where unimpeded, ctenostomes spread quickly over open shell surface by rapid stolon growth.

Early transitions seem to have resulted from a kind of facilitation in which ctenostomes in some way modified or prepared shell substrata for colonization by varied borers and epilithic cheilostomes. Colonizing propagules of a variety of organisms may have sought substrata already infested by living ctenostomes, or may have selected surfaces riddled with abandoned tunnels and pores of dead ctenostomes. Relative importance of intermediate stage bionts could have depended as much on availability of propagules as on any interspecific competitive hierarchy, but the fine-structure of these middle steps has been only very roughly resolved. Later stages seem to have resulted from the space-competitive superiority of encrusting colonial organisms over non-colonial bionts (Jackson, 1977), and from a mechanism akin to the tolerance model of Connell and Slatyer (1977) in which a combination of slow growth rate, persistent colony expansion, and ability to gradually overgrow other bionts permitted eventual dominance by epilithic cheilostomes.

This shell substratum microsuccession is similar to that described by paleontologists and marine ecologists studying community development on cobbles and boulders, with low biont diversity in early stages, high diversity in middle stages, ending with dominance by one or two superior space-competitors. The transition sequence can be "reset" by disturbance that diminishes or removes the species dominating later stages (Figures 5B, C, D). It is worth noting that in a study of Ordovician cobble-dwelling organisms a generally similar succession was observed, which also included early "vinelike" bryozoans, diverse middle stages, and a final stage dominated by an epilithic bryozoan (Wilson, 1985, Fig. 2 and Table 1). Although the taxonomic staffing of fouling communities has changed through time, especially as a result of radiations of endobenthic organisms in the Mesozoic and Cenozoic (Vermeij, 1987), the general pattern of localized biont transitions may have remained virtually unchanged.

ACKNOWLEDGMENTS

I thank Alan H. Cheetham for identification of bryozoans. Nancy Walters helped with processing of samples and Carolyn Young typed the manuscript. Fieldwork was supported by Sigma Xi (Tulane University Chapter) and Geological Society of America. Special thanks go to Lauck W. Ward and Victor A. Zullo for commenting on the manuscript.

REFERENCES

Bailey, R.H., and Tedesco, S.A., 1986, Paleoecology of a Pliocene coral thicket from North Carolina: an example of temporal change in community structure and function: Jour. Paleont., v. 60, p. 1159-1176.

Blackwelder, B.W., 1981, Late Cenozoic marine deposition in the United States Atlantic Coastal Plain related to tectonism and global climate: Palaeogeogr., Palaeoclimat., Palaeoecol., v. 34, p. 87-114.

Boekschoten, G.J., 1970, On bryozoan borings from the Danian at Fakse, Denmark, *in* Crimes, T.P., and Harper, J.C., eds., Trace Fossils: Seel House Press, Liverpool, p. 43-48.

Bromley, R.G., 1970, Borings as trace fossils and *Entobia cretacea* Portlock, as an example, *in* Crimes, T.P., and Harper, J.C., eds., Trace Fossils: Seel House Press, Liverpool, p. 49-90.

Connell, J.H., and Keough, M.J., 1985, Disturbance and patch dynamics of subtidal marine animals on hard substrata, *in* Pickett, S.T.A., and White, P.S., eds., The Ecology of Natural Disturbance and Patch Dynamics: Academic Press, Orlando, p. 125-151.

Connell, J.H., and Slatyer, R.O., 1977, Mechanisms of succession in natural communities and their role in community stability and organization: Am. Natural., v. 111, p. 1119-1144.

Cronin, T.M., Bybell, L.M., Poore, R.Z., Blackwelder, B.W., Liddicoat, J.C., and Hazel, J.E., 1984, Age and correlation of emerged Pliocene and Pleistocene deposits, U.S. Atlantic Coastal Plain: Palaeogeogr., Palaeoclimat., Palaeoecol., v. 47, p. 21-51.

DuBar, J.R., Howard, J.F., 1969, Paleoecology of the James City Formation (Plio-Pleistocene?), Neuse River estuary, North Carolina: Geol. Soc. Am., Abstracts with Programs, part 4, p. 20.

DuBar, J.R., Solliday, J.R., and Howard, J.F., 1974, Stratigraphy and morphology of Neogene deposits, Neuse River estuary, North Carolina, *in* Oaks, R.Q., and DuBar, J.R., eds., Post-Miocene Stratigraphy, Central and Southern Atlantic Coastal Plain: Utah State Univ. Press, Logan, p. 102-122.

Fretter, V., and Graham, A., 1962, British Prosobranch Molluscs: Ray Society, London, 755 pp.

Jackson, J.B.C., 1977, Competition on marine hard substrata: the adaptive significance of solitary and colonial strategies: Am. Natural., v. 111, p. 743-767.

Jackson, J.B.C., 1983, Biological determinants of present and past sessile animal distributions, *in* Tevesz, M.J.S., and McCall, P.L., eds., Biotic Interactions in Recent and Fossil Benthic Communities: Plenum Press, New York, p. 39-120.

Kidwell, S.M., and Jablonski, D., 1983, Taphonomic feedback: ecological consequences of shell accumulation, *in* Tevesz, M.J.S., and McCall, P.L., eds., Biotic Interactions in Recent and Fossil Benthic Communities: Plenum Press, New York, p. 195-248.

Miller, W., III, 1986, Paleoecology of benthic community replacement: Lethaia, v. 19, p. 225-231.

Miller, W., III, 1987, Community replacement in two mollusk-dominated fossil sequences, Pleistocene of North Carolina: Am. Malacol. Union, Program with Abstracts, p. 15.

Miller, W., III, in press, Checklist of megafossils from the James City Formation (lower Pleistocene) at Johnson Point, Craven County, North Carolina: Tulane Stud. Geol. Paleont.

Miller, W., III, and DuBar, J.R., 1988, Community replacement of a Pleistocene *Crepidula* biostrome: Lethaia, v. 21, p. 67-78.

Reading, H.G., ed., 1978, Sedimentary Environments and Facies: Elsevier, New York, 557 pp.

Selley, R.C., 1969, Studies of sequence in sediments using a simple

mathematical device: Quat. Jour. Geol. Soc. London, v. 125, p. 557-581.
Sousa, W.P., 1985, Disturbance and patch dynamics on rocky intertidal shores, *in* Pickett, S.T.A., and White, P.S., eds., The Ecology of Natural Disturbance and Patch Dynamics: Academic Press, Orlando, p. 101-124.
Wilson, M.A., 1985, Disturbance and ecologic succession in an Upper Ordovician cobble-dwelling hardground fauna: Science, v. 228, p. 575-577.
Woods, D.M., 1987, The paleoecology of *Crepidula* (Gastropoda) beds, James City Formation (Pleistocene), North Carolina: Unpubl. M.S. thesis, Tulane Univ., New Orleans, 119 pp.
Vermeij, G.J., 1987, Evolution and Escalation: Princeton Univ. Press, 527 pp.
Zullo, V.A., and Miller, W., III, 1986, Barnacles (Cirripedia:Balanidae) from the lower Pleistocene James City Formation, North Carolina, with the description of a new species of *Balanus* da Costa: Proc. Biol. Soc. Washington, v. 99, p. 717-730.